frontiers in Earth Science

ORIGINAL RESEARCH
published: 28 January 2021
doi: 10.3389/feart.2020.602870

# Petrogenesis of Mesoproterozoic Granites of the Swartoup Hills Region, Kakamas Domain, Namaqua Belt, South Africa

*Steffen Hermann Büttner, Stephen Anthony Prevec* and Graeme Alvin Schmeldt*

*Department of Geology, Rhodes University, Makhanda (Grahamstown), South Africa*

The Swartoup and Polisiehoek plutons in the Swartoup Hills (South Africa) formed during an episode of significant magma emplacement in the Mesoproterozoic Namaqua Sector of the Namaqua Metamorphic Province. They intruded into mid-crustal metasedimentary rocks of the metapelitic Koenap and mafic to carbonate-bearing Bysteek Formations during and shortly after the ~1,200–1,220 Ma regional metamorphic peak that reached ultrahigh temperatures. Subsequent to pluton emplacement, the crust underwent regional high-temperature deformation during slow near-isobaric cooling. A further episode of pluton emplacement associated with fluid circulation truncated the first-order regional tectonic structures at ~1,100 Ma. Based on their petrography, the Swartoup pluton is subdivided into leuco-granitoids with biotite as the sole mafic phase, pyroxene granitoids, and garnet-bearing granitoids, which may contain significant biotite. These subgroups display distinctive geochemical variations from one another, and from the Koenap Formation migmatites and the Polisiehoek granites, which are exposed nearby. Incompatible trace element distributions suggest that the Swartoup and Polisiehoek granitoids represent modified A-type granite magma, consistent with derivation from partial melting of quartzo-feldspathic crust. The magmas incorporated significant amounts of juvenile mantle-derived magma ($\varepsilon_{Nd}{}^{1200}$ of ~−5, and LREE-depleted), but do not require older, early to late Paleoproterozoic crust. Particularly close to contacts to the calcic Bysteek Formation, localized contamination of the Swartoup granites by supracrustal carbonates is evident. A relatively pervasive alkali metasomatic effect is manifested strongly in the initial $^{87}Sr/^{86}Sr$ and LILE profiles of the Polisiehoek granites in particular, as well as in some of the Swartoup pyroxene granitoids, which could be either a symptom of $CO_2$ metasomatism related to the Bysteek Formation carbonates, or to post-magmatic fluid metasomatism, perhaps linked to regional shearing. The comparison of our results with literature data suggests that similar sources, A-type granitic, Meso- to Paleoproterozoic crustal, and enriched mantle, have contributed, in locally differing proportions, to granites in most parts of the Namaqua Sector. Most likely, these plutons were generated during crustal and mantle melting in a long-lived hot continental back-arc environment.

**Keywords: A-type granite, migmatite, melt mixing, Kakamas Domain, radiogenic isotopes, Proterozoic crust**

OPEN ACCESS

***Edited by:***
*Steven W. Denyszyn, University of Western Australia, Australia*

***Reviewed by:***
*J. Gregory Shellnutt, National Taiwan Normal University, Taiwan*
*Kwan-Nang Pang, Academia Sinica, Taiwan*
*Jaroslav Dostal, Saint Mary's University, Canada*

****Correspondence:***
*Stephen Anthony Prevec*
*s.prevec@ru.ac.za*

***Specialty section:***
*This article was submitted to Petrology, a section of the journal Frontiers in Earth Science*

***Received:*** *04 September 2020*
***Accepted:*** *16 November 2020*
***Published:*** *28 January 2021*

***Citation:***
*Büttner SH, Prevec SA and Schmeldt GA (2021) Petrogenesis of Mesoproterozoic Granites of the Swartoup Hills Region, Kakamas Domain, Namaqua Belt, South Africa. Front. Earth Sci. 8:602870. doi: 10.3389/feart.2020.602870*

## INTRODUCTION

During its formation and evolution, granitic magma may be exposed to processes and factors that influence its mineral, chemical, and isotope composition, grain size, texture, and contact relationships with the host rocks into which the pluton is emplaced and where it solidifies. These parameters include the variably homogenous or heterogeneous source rocks from which the granite magma is generated, the lithospheric level in which the primary magma is formed, and the contribution of different magmas that may mix or mingle during ascent or emplacement (e.g., Vernon et al., 1988; Baxter and Feeley, 2002). Assimilation of, and chemical reaction with, host rocks may contaminate granitic magma, causing local compositional and textural variations (e.g., Clemens et al., 1986; Clemens and Vielzeuf, 1987; Clemens, 2003; Chappell et al., 2004; Clemens and Stevens, 2012). The extent of interaction that is possible with the host rock depends on further factors, such as the mineral composition of the host rock, its temperature and physical state, and the capacity of the intruding magma to react with the host rock, depending on the composition, shape, size, and temperature of the magma chamber.

The petrogenetic importance of each of these parameters and processes can be identified and evaluated *via* the analysis of the mineralogical and geochemical variability of the chemical and isotopic compositions of the pluton, the field relationships between pluton and host rocks, comparison with other plutons of equal age nearby, and the understanding of the evolution of the crust hosting these plutons (Clarke, 1992).

The crustal evolution of the Namaqua Metamorphic Province in South Africa and Namibia (**Figure 1A**) is characterized by a long-standing high-temperature regime in the Mesoproterozoic, particularly between ~1,230 and ~1,080 Ma, with further episodes of early (~1,300 Ma) and late (~1,000 – 1,030 Ma) magmatism in some parts of the belt (Robb et al., 1999; Raith et al., 2003; Clifford et al., 2004; Bial et al., 2015a; Bial et al., 2015b; Abrahams and Macey, 2020; Groenewald and Macey, 2020). Granitic to charnockitic plutonism is predominant and widespread

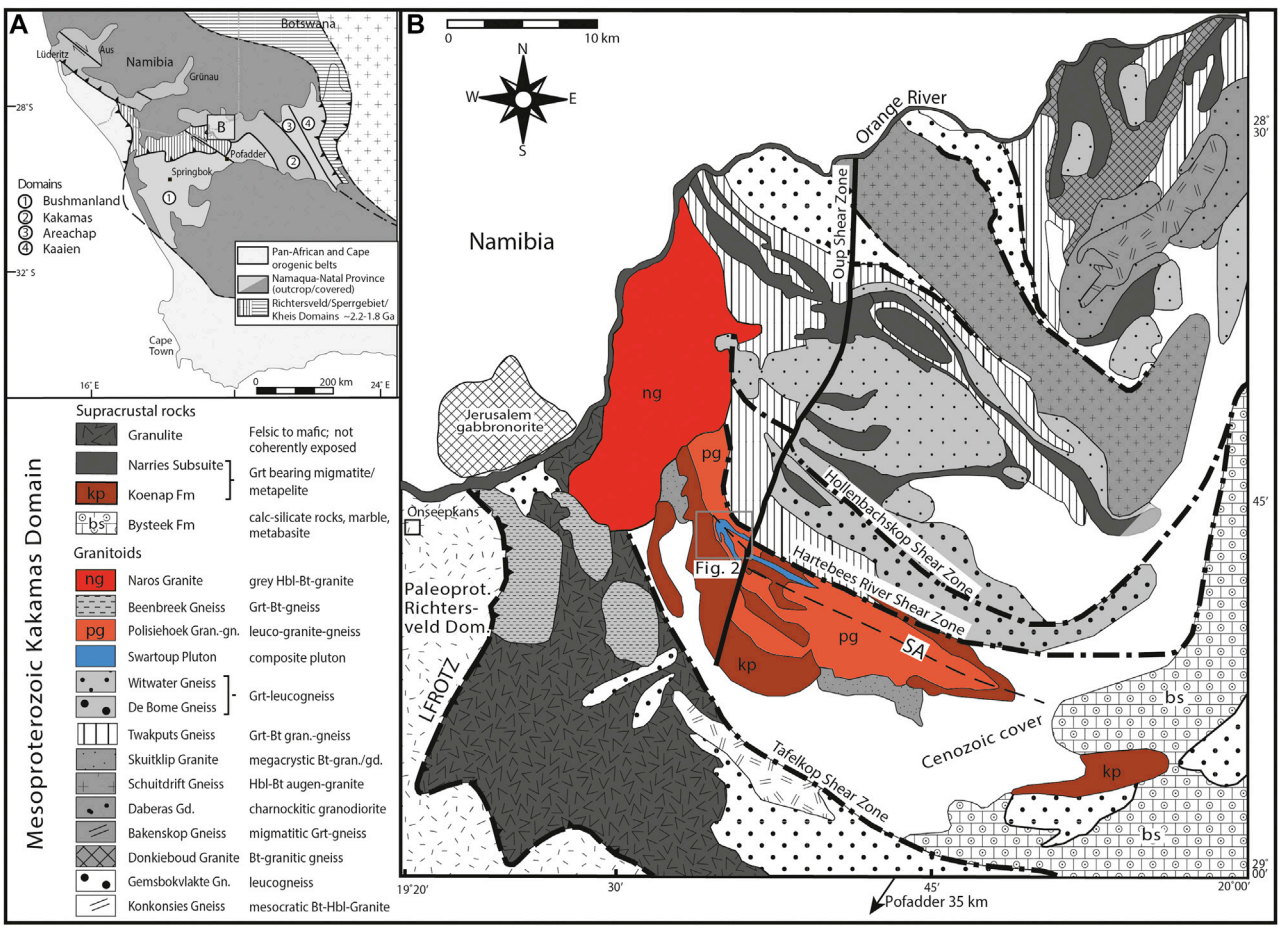


**FIGURE 1 |** Regional geology of the Namaqua Sector of the Namaqua-Natal Metamorphic Province. **(A)**. The four Mesoproterozoic domains of the Namaqua Sector and the Palaeoproterozoic basement of the Richtersveld, Sperrgebiet, and Kheis Domains in southwestern Africa. **(B)** The central Namaqua Sector in South Africa with its main granitic and supracrustal entities and regional shear zones. Along the Lower Fish River-Onseepkans Shear Zone (LFROTZ; Macey et al., 2015), the rocks of the Kakamas Domain are thrusted over the Paleoproterozoic Richtersveld Domain. The position of the map in **Figure 2** is highlighted. Maps A and B are modified after Bial et al. (2015b) and references therein. SA: Swartmodder antiform.

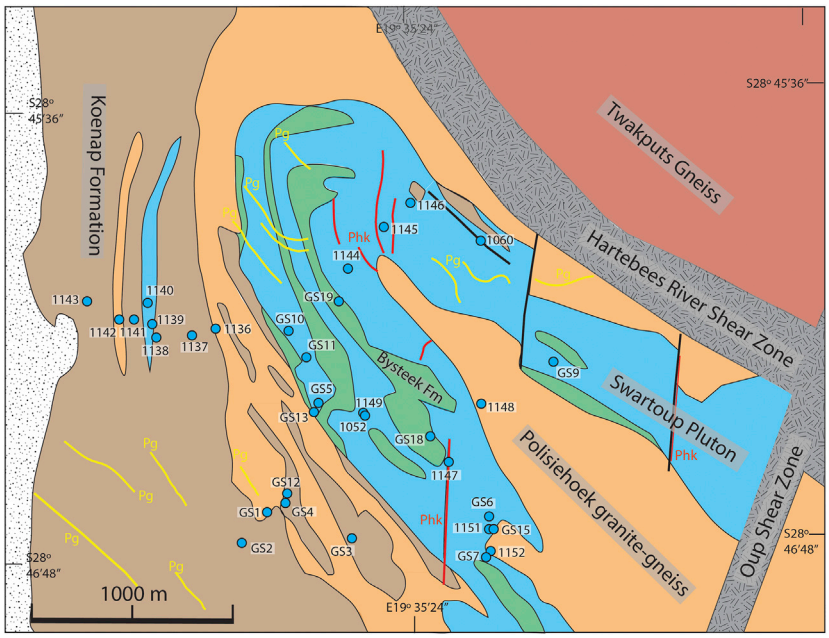


**FIGURE 2 |** Simplified geological map of the study area (**Figure 1B**) showing the distribution of lithological entities, main structures, and sample locations. Pg, pegmatites (in yellow); Phk, Polisiehoek Granite dykes (in red). Pegmatites are post-orogenic and undeformed. Polisiehoek Granite dykes commonly show sheared boundaries or, in some places, penetrative mylonitization.

throughout the orogen. Mafic or bimodal magmatism, such as the Jerusalem gabbronorite (**Figure 1B**), the Kum-Kum norite, and the Tantalite Valley Complex (Miller, 2008), emplaced between ~1,210 and 1,225 Ma (unpublished data; pers. comm. Paul Macey, 2020), basaltic lavas in the Bushmanland Group (~1,130 ± 35 Ma; Cornell et al., 2009), the ~1,100 Ma Koras Group (Bailie et al., 2012), or the ~1,030 Ma Koperberg Suite (Clifford et al., 1995; Robb et al., 1999), indicate fertile mantle sources throughout much of the evolution of the lithosphere in the Namaqua Sector.

The tectonic setting of the Namaqua Metamorphic Province, particularly its Namaqua Sector (**Figure 1**), is a matter of debate. The traditional model developed in the 1980s (Joubert, 1986; Stowe, 1986; and reviewed by Miller, 2012) proposes multiple oceanic basins separating small continental fragments in the early Mesoproterozoic, presuming multiple subduction zones and eventual terrane collisions at ~1,200 Ma in the context of Rodinia assembly. More recently, this model has been challenged (Bial et al., 2015a; Bial et al., 2015b; Macey et al., 2016; Büttner, 2020), particularly on the basis of the lack of convincing indicators for subduction- or collision-related metamorphism, or evidence for the existence of oceanic basins once separating crustal entities in the region at that time. Bial et al. (2015a) proposed a long-lived continental back-arc, with regionally and chronologically variable heat and magma transfer into thin lithosphere, as the most likely tectonic setting for the Namaqua Sector in the Mesoproterozoic. Although the Namaqua Metamorphic Province evolved in the time period during which Rodina formed, there appears to be no evidence that the Namaqua Sector was involved in the collision of pre-Rodinia cratons or lithospheric fragments, and it may well have formed along the margin of the evolving supercontinent.

Granite petrogenesis is a monitor of processes during the high-temperature episodes in the Namaqua Sector, and a number of studies, particularly by Bailie (Bailie et al., 2010; Bailie et al., 2012; Bailie et al., 2017; Bailie et al., 2019), have used the geochemistry and isotopic signatures of granitoid rocks for the interpretation of the regional crustal evolution. The current study adds new complementary data from the Swartoup and Polisiehoek plutons in the central part of the Namaqua Sector, in the Kakamas Domain (**Figures 1A,B**).

In the field, the Swartoup Pluton (**Figure 1B**) shows compositional heterogeneity and locally significant metasomatic or magmatic interaction with pelitic and calcic host rocks of the supracrustal Koenap and Bysteek Formations, indicated by transitional contacts or hybrid rock types. By contrast, the spatially associated Polisiehoek granite gneiss, which according to crosscutting relationships is younger than the Swartoup Pluton, shows sharp boundaries with the Swartoup Pluton and the supracrustal host rocks along pluton and dyke contacts. At the scale of hundreds of meters (**Figure 2**), both, the Swartoup and the Polisiehoek plutons intrude the Bysteek and the Koenap Formations along irregular contacts, forming lenses of host rock within the plutons. These lenses show compositions, structural trends, and shapes that are compatible with the regional geological structure and lithology, and therefore are most likely roof pendants.

In this study, we investigate the field relationships, the compositional and geochemical variations, and Nd and Sr isotope signatures of the Swartoup and Polisiehoek plutons

and their host rocks. We discuss potential magma sources, petrogenetic processes, and possible genetic relationships, and the extent and nature of interactions between intrusive magma and host rocks, in the context of the regional evolution of the Mesoproterozoic crust. The compositional variations of these plutons are compared with data from other parts of the Namaqua Sector, and their petrogenesis is evaluated in the context of the tectonic setting of the region in Mesoproterozoic time.

## Geological Context and Regional Crustal Evolution

The Mesoproterozoic Kakamas Domain (**Figure 1**) consists of medium- to high-grade metamorphic supracrustal metamorphic rocks which commonly show extensive anatexis. Predominantly granitoid plutons intruded this basement between ~1,220 and ~1,180 Ma, and in a second episode at ~1,100 Ma (Bial et al., 2015a; Bial et al., 2015b). The region of the Swartoup Hills, east of the Lower Fish River-Onseepkans Thrust Zone (LFROTZ; **Figure 1B**), along which the Kakamas Domain has been thrusted over the Paleoproterozoic Richtersveld Magmatic Arc in the west (Thomas et al., 2016; Macey et al., 2017) is arguably the highest grade metamorphic region within the Kakamas Domain. In this area, the Swartoup and Polisiehoek plutons and their metamorphic host rocks formed and developed in a high- to ultrahigh temperature (HT/UHT) and low-pressure environment reaching up to about 900°C, at pressures not exceeding 500–550 MPa (Bial et al., 2015a; Bial et al., 2015b). Spinel–quartz– and osumilite-bearing parageneses in felsic host rocks indicate the UHT increment of the P–T path. Regional anatexis and diatexis in rocks of pelitic and psammopelitic bulk composition are associated with the thermal maxima (Bial et al., 2015a).

The ages of magmatic zircon in migmatites indicate two episodes of anataxis in the metamorphic basement in the region, an early phase around ~1,300–1,350 Ma and a second phase around 1,200 Ma (Bial et al., 2015a). It is not evident which of these episodes is responsible for the growth of the UHT mineral assemblages, but Bial et al. (2015a) consider the ~1,200 Ma anataxis as the dominant melt-forming episode in the supracrustal rocks of the region.

The metamorphic history is characterized by slow isobaric cooling over at least ~120 m.y. between ~1,200 Ma to 1,070–1,090 Ma that alternates with episodic reheating, but only minor pressure variation. For this time period, there is no indication of temperatures of metamorphism of less than upper amphibolite facies conditions or pressure increments higher than 550 MPa. In the Aus region of Namibia (**Figure 1A**), the crust of the Kakamas Domain reached high temperature and low pressure conditions associated with granitic plutonism much later, at about 1,030 – 1,060 Ma (Diener et al., 2013). At this time, the crust in the Swartoup Hills already had cooled down to lower amphibolite facies conditions (Büttner et al., 2013). The most likely tectonic setting of this long-lasting high-temperature/low-pressure evolution with episodic plutonism and thermal peaks is the thin and hot lithosphere of a Mesoproterozoic continental back-arc (Bial et al., 2015a; Büttner, 2020).

The long-lasting high-temperature metamorphic history of the Swartoup Hills region correlates in time with two main episodes of crustal plutonism, an earlier one at 1,230–1,180 Ma during regional anatexis, and a later pronounced event at ~1,100 Ma, during which one of the largest bodies in the region, the Naros pluton, was emplaced (Bial et al., 2015b; Macey et al., 2015; Macey et al., 2016).

The main episode of crustal deformation is bracketed by the ages of regional anataxis and pluton emplacement episodes. The dominant structural inventory consists of large-scale dome-and-basin structures and regional ductile shear zones (Moen and Toogood, 2007). Both structure types overprint migmatites and the ~1,200 Ma plutons, but the ~1,101 Ma Naros pluton truncates regional dome-and-basin structures and the main shear zones, such as the Hartebees River or the Hollenbachskop shear zones (**Figures 1B**, **2**; Bial et al., 2015a; Bial et al., 2015b). Locally, magmatic foliation suggests the late-tectonic emplacement of the Naros pluton (Bial et al., 2015b). A similar situation exists further east along the Hartebees River shear zone, where the Karama'am Granite (1,106 ± 8 Ma) truncates its mylonitic structure (Colliston et al., 2015). For the Grünau area in neighboring Namibia, Bial et al. (2016) provide a more accurate estimate of the time of deformation along regional shear zones. In the Grünau shear zone, a younger monazite generation, compositionally distinct compared to monazite related to the regional ~1,200 Ma metamorphic peak, formed between ~1,130 and 1,120 Ma. This age is interpreted to date the mylonitization along this shear zone (Bial et al., 2016). The same age of 1,125 ± 5 Ma is found in zircon rims, interpreted as high-temperature growth in the solid state in granites nearby major shear zones, such as the 1,195 ± 16 Ma Skuitklip Granite (Bial et al., 2015b; **Figure 1B**). The Polisiehoek granite gneiss has been dated as 1,203 ± 11 Ma (Pettersson, 2008), with a $T_{DM}$ age of 2,244 Ma indicating a significant Paleoproterozoic component in its source (Pettersson et al., 2009).

In the wider area of the Swartoup pluton, Bial et al. (2015b) identify three distinct groups of granitoid plutons: 1) mesocratic granites, 2) leucocratic granites, and 3) leucogranites. Mesocratic granitoids are high-K, ferroan granites and tonalities, enriched in large-ion lithophile elements (LILEs) and rare-earth elements. They characterized these plutons as A- and I-type granitoids (e.g., Whalen et al., 1987; King et al., 1997; Zhang et al., 2019). Bial et al. (2015b) proposed that these granites formed by fractional crystallization of a hot (~900°C), mafic parental magma. The leucocratic granitoids and leucogranites vary from granitic to syenitic compositions, and were interpreted as products of low temperature (<730°C), fluid-present partial melting of a felsic metasedimentary source, classifying them as S-type granitoids. All mesocratic and leuco-/leucocratic granitoids, except the ~1,101 Ma Naros granodiorite, were emplaced between ~1,220 and ~1,180 Ma (Bial et al., 2015b). Mafic and ultramafic plutons in southernmost Namibia intruded between ~1,225 and 1,210 Ma (Paul Macey, unpublished data, pers. comm., 2020). Accordingly, for this time frame, both the crust and the mantle must be considered possible sources for granitoid plutonism. At the

same time, major anataxis affected the pluton-hosting supracrustal rocks (Bial et al., 2015a), which created the possibility of anatectic melt contributing to the formation of plutons in the Kakamas Domain. Given a period of regional magmatic zircon growth in metamorphic rocks between ~1,225 and ~1,175 Ma (Bial et al., 2015a), an age bracket for the metamorphic peak in the Koenap migmatites of ~1,200 ± 25 Ma can be proposed.

Following a protracted period of high crustal temperatures, a second heat pulse around 1,100 Ma facilitated zircon growth in older plutons and production of the younger granite suite (Naros pluton, the Donkieboud Granodiorite, and smaller bodies such as the Beenbreek pluton; Pettersson, 2008; Bial et al., 2015b; Abrahams and Macey, 2020). This renewed plutonic activity around 1,100 Ma is associated with reheating of the crust and fluid circulation, manifested in the renewed growth of monazite and garnet (Bial et al., 2015a). Crustal cooling below mid-amphibolite facies conditions took at least an additional 75–115 m.y. Such crustal temperatures in the Swartoup Hills area are estimated for ~985–1,026 Ma (Pettersson, 2008; Büttner et al., 2013; Bial et al., 2015a).

## ANALYTICAL METHODS

A total of forty-four representative rock samples were collected from the study area: ten from the Koenap Formation migmatites, three from the Bysteek Formation, twenty-one from the Swartoup Pluton, and nine from the Polisiehoek granite gneisses. Sampling localities are shown in **Figure 2**.

Major elements were determined by XRF analysis at the Central Analytical Facility at Stellenbosch University (South Africa) on fused glass discs using a PANalytical Axios wavelength dispersive spectrometer. The spectrometer utilized a 2.4-kW Rh-tube and LIF200, LIF220, PE 002, Ge 111, and PX1 crystals, and used a gas-flow (90% argon–10% methane gas mixture) proportional counter and a scintillation detector. Matrix effects in the samples were corrected for using theoretical alpha factors and measured line overlap factors using SuperQ PANalytical software. Calibration standards included the NIM-G (granite from the Council for Mineral Technology, South Africa) and BE-N (basalt from the International Working Group). Trace element analysis was conducted on the same fused discs by LA-ICP-MS at the same facility, using a Resonetics 193 nm excimer laser connected to an Agilent 7700 ICP-MS. Trace elements are quantified using NIST612 for calibration and the silica content from XRF as an internal standard, and BCR-2 and BHVO 2G as external standards. Duplicate measurements were made on each sample.

Rb/Sr and Sm/Nd isotopic ratios were measured for twenty-seven samples using Nu Instruments HR MC-ICP-MS at the University of Cape Town, South Africa, using the methods described by Harris et al. (2015). For strontium, the reference granite standard JG-2 gave a value of $^{87}Sr/^{86}Sr = 0.76014 \pm 3$, consistent with the internal reproducibility of 0.760 ± 1 (n = 6), compared to a literature reported value of ~0.75805 (Ma et al., 2013). Strontium isotope compositions were corrected for Rb interference and normalized to $^{86}Sr/^{88}Sr = 0.1194$ to correct for thermal fractionation. For Nd, analyses were monitored relative to a standard value for JG-2 of $^{143}Nd/^{144}Nd = 0.512250 \pm 12$, as compared to an internal value of 0.512232 ± 24 (n = 17) and a literature value of ~0.51221 (e.g., Miyakazi and Shuto, 1998). Mass interference from Sm was corrected based on natural Sm isotopic composition, and thermal fractionation of Nd isotopic composition was corrected during analysis by normalization to $^{146}Nd/^{144}Nd = 0.7219$.

## OBSERVATIONS AND ANALYTICAL DATA

### Field observations and field relationships of the Swartoup Pluton, the Polisiehoek granite gneiss, and their host rocks

#### Swartoup Pluton

The Swartoup Pluton forms a narrow, up to 600-m thick plutonic layer that stretches approximately 10 km along strike (**Figure 1B**). Subsequent folding in its solid state affected the pluton and its host rocks, producing a first-order NW-SE trending and NE plunging antiformal structure, to which Moen and Toogood (2007) refer as the Swartmodder antiform (**Figure 1B**). Localized ductile deformation formed mylonite or ultramylonite zones up to ~1 m thick in the Swartoup Pluton. Away from these zones, the pluton shows macroscopically undeformed granitic texture and, in some places, minor magmatic foliation.

The pluton consists of different lithological varieties including granites, granodiorites, and less commonly, monzonites, quartz-monzonites, and monzo-diorites. Orthopyroxene is rare and in the current study has been found in only one location in a monzo-diorite (Loc. 1,151; **Figure 2**), allowing the classification as enderbite. Bial et al. (2015b) describe another occurrence, but these rocks appear to form only a small proportion of the pluton. Alkali feldspar phenocrysts, typically between 0.5 and 2.5 cm in size are, irrespective of the extent of weathering, visible in most parts of the Swartoup Pluton (**Figure 3A**), suggesting that the most abundant rock type is granodiorite or granite. In addition to quartz and the feldspars, the mineralogy of the Swartoup Pluton typically consists of biotite and accessory phases such as apatite and zircon. Garnet is typically rare, but can be locally abundant, and pyroxene is typically absent. The rocks are medium- to coarse-grained and, where fresh, medium to dark gray. The boundaries between the different granitoid varieties are often not exposed or are masked by weathering. Where they are exposed, they are gradational, suggesting coexistence of different granitoid magmas.

The 1:250,000 geological map of the region shows the Swartoup Pluton as "Swartoup Enderbite" (Moen and Toogood, 2007). However, since orthopyroxene-bearing tonalitic material is present in only a few small domains of the pluton, and overwhelmingly the pluton is alkali feldspar-rich and mostly pyroxene-free, we deem the name "Swartoup Pluton" more appropriate for this intrusion.

Close to, and in contact with, the calcic rocks of the Bysteek Formation, the Swartoup Pluton grades into a several meter thick zone of clinopyroxene-rich granodiorites, granites, and tonalites that contain variable amounts of alkali feldspar, plagioclase, and quartz. Plagioclase phenocrysts may reach up to 4 cm in size. The dominant morphotype is a leucocratic feldspathic granitoid, but it can be locally melanocratic and/or gneissose, with leucosome


**FIGURE 3 |** Field appearance of the Swartoup and Polisiehoek plutons and their host rocks. **(A)** Alkali feldspar-rich Swartoup leucogranite from the interior of the pluton with undeformed magmatic texture. **(B)** Magmatic megabreccia in mafic granulites of the Bysteek Formation. The intruding facies of the Swartoup Pluton is leucocratic and may be alkali feldspar or plagioclase dominated, but always shows large magmatic clinopyroxene. This type of granitoid is restricted to the contact zone of the Swartoup pluton with the metabasites of the Bysteek Formation. Inset: Centimeter-sized magmatic clinopyroxene in leucocratic matrix at the contact to a fine-grained metabasite fragment. Gradational contacts indicate the interaction of the intruding magma with the breccia clasts. **(C)** Dyke of Polisiehoek Granite cutting the Swartoup Pluton at sharp intrusive boundaries. Elswhere, such contacts are commonly sheared. **(D)** Convoluted folding of marble and calc-silicate rock layers of the Bysteek Formation. **(E)** Stromatic to nebulitic migmatite of the Koenap Formation with abundant garnet in alkali feldspar-rich leucosome. Cordierite and sillimanite, or biotite are commonly present. **(F)** Alkali feldspar phenocrystic Swartoup Pluton overprinted during regional deformation at high temperature along a shear zone parallel to the Hartebees River shear zone (Loc. 1,060; **Figure 1B**).

veins, and significant accessory clinopyroxene (the latter as distinctive phenocrysts up to 2 cm in diameter; **Figure 3B**), or garnet present. This rock type is therefore distinguished from the homogeneous granitoids with biotite as the sole mafic mineral that typifies the Swartoup Pluton rocks. Accordingly, three petrologic based subtypes of the Swartoup intrusion are designated in this study, consisting of 1) Swartoup leucogranitoids, which are the quartzo-feldspathic, felsic granitoids with biotite as the sole mafic phase; 2) Swartoup pyroxene granitoids, which are typically more melanocratic, and contain clinopyroxene except in sample 1,151 that contains orthopyroxene; and finally 3) Swartoup garnet granitoids, which contain macroscopically visible garnet present in variable but in places significant quantity. Where the Swartoup Pluton intrudes the metabasites of the Bysteek Formation, up to meter-sized angular clasts of mafic granulites and the Swartoup clinopyroxene granitoid form distinctive magmatic mega-breccias with macroscopically evident interaction between intruding magma and granulite fragments are observed (**Figure 3B**).

### Polisiehoek Granite Gneiss

The Polisiehoek granite gneiss is one of the largest plutons in the region, with an outcrop size of ~40 × 8 km (**Figure 1**). It is a largely uniform leucocratic rock with medium- to coarse-grained alkali feldspar and quartz as the dominant phases, minor plagioclase, and in places some garnet. Biotite is rare or absent. Significant ductile deformation formed up to several hundred-meter-thick zones with a characteristic penetrative continuous schistosity, particularly in an area immediately to the southwest of the boundary between Polisiehoek gneiss and the Swartoup Pluton (**Figure 2**). On foliation planes, transport lineations are rare, suggesting deformation predominantly in the oblate field of strain. In such zones, the magmatic mineral assemblage is entirely recrystallized with alkali feldspar grain sizes of 100–400 μm, but small rheological contrasts between feldspar and quartz prevent the formation of augen-shaped clasts. Other areas in the Polisiehoek granite gneiss remained undeformed and show medium- to coarse-grained magmatic textures without significant flow textures. The pink alkali feldspar in undeformed Polisiehoek granite dominates the color of the rock in the field. In sheared domains, the recrystallized alkali feldspar is white. Weathering and minor iron oxide or hydroxide precipitation in the sheared domains is characterized by its orange weathering color, which is an indicative and obvious feature of the Polisiehoek granite gneiss in the field.

The Polisiehoek granite gneiss forms the core and the outer margin of the Swartmodder antiform (**Figures 1B**, **2**), which indicates its pre-tectonic emplacement and its intrusion on either side of the Swartoup Pluton layer. Prominent Polisiehoek granitic dykes, up to ~2 m thick, crosscut the Swartoup Pluton (**Figure 3C**), indicating the relative age relationship of the two plutons. Some connect the inner and outer Polisiehoek granite layers of the Swartmodder antiform. Commonly, but not always, the dyke margins are intensely sheared in the solid state, causing mylonites and ultramylonites to form.

Along the northeastern limb of the Swartmodder antiform, shearing along the Hartebees River Shear Zone (HRSZ; **Figures 1B**, **2**) overprints the Polisiehoek granite gneiss, and, less commonly, parts of the Swartoup Pluton and the supracrustal host rocks. The HRSZ offsets the lithological sequence, juxtaposing the rock sequence that is the focus of the current study with the Twakputs gneiss to the northeast of the shear zone (**Figures 1B**, **2**). The Twakputs gneiss formed as an in situ low-temperature S-type granite (Bial et al., 2015b).

### Supracrustal Rocks: Koenap and Bysteek Formations

Metapelitic diatexites of the Koenap Formation and granulite-facies calc-silicates, marbles, and metabasites of the Bysteek Formation (**Figures 3B,D**) form the immediate host rocks of the Swartoup and Polisiehoek plutons (**Figure 2**). The protolith ages of these supracrustal metamorphic host rocks are not accurately known. Moen and Toogood (2007) deem the Bysteek Formation stratigraphically older than the Koenap Formation, but due to the intense deformation and metamorphism in the region, this age relationship could not be verified in the field. Common inherited Paleoproterozoic (~1.8–2.0 Ga) and early Mesoproterozoic zircon (Moen and Toogood, 2007), in some cases showing indication of detrital transport (Bial et al., 2015a; Bial et al., 2015b), indicate the Paleoproterozoic heritage and possible sediment sources of that age. Moen and Toogood (2007) estimate the depositional age of the Koenap Formation's protolith as between 1.3 and 1.8 Ga.

The carbonate, calcic-pelitic, and pelitic composition of the Bysteek and Koenap Formations suggest variable, gradually changing deposition of carbonate grading into marls and eventually psammopelitic/pelitic material. Moen (2001) emphasizes the transitional nature of the carbonatic Bysteek and pelitic/psammopelitic Koenap Formations. Accordingly, the metabasites of the Bysteek Formation may have formed either from marls or mafic igneous protoliths. In the study area, the Bysteek Formation forms only narrow outcrops that form contacts with the Koenap Formation and both plutons (**Figure 2**). The main outcrop of the Bysteek Formation is 20–50 km to the southeast of the study area (**Figure 1B**).

The Koenap Formation forms topographic highs as small hills of several tens of meters in diameter within the intrusive Polisiehoek granite gneiss but forms coherent basement further to the southwest (**Figures 1B**, **2**). A black oxide layer of desert varnish disguises the typically lighter color of the fresh rocks. The Koenap Formation shows a variety of high-grade metamorphic rocks ranging from stromatic to nebulitic migmatites (**Figure 3E**), diatexites, and pockets of in situ granite. Moen and Toogood (2007) refer to these rocks as "kinzigites." In other domains, the migmatites and diatexites grade into homogenous medium-grained gray granofelsic granulites without layering or separation of leucocratic and mafic material. Their composition and texture is consistent with that of restitic felsic granulite.

Leucosome dykes, up to decimeter thickness, transecting the layering in stromatic migmatites along diffuse and gradual boundaries suggest some melt mobility during anatexis. In some places, such dykes are connected to granitic pools of several meters in diameter. However, there is no indication that such dykes have transported magma over larger distances (e.g., tens or hundreds of meters) or in large volumes.

The composition of the anatexites and granulites of the Koenap Formation consists of quartz, alkali feldspar, plagioclase, garnet, and minor cordierite, sillimanite, biotite, and spinel. Plagioclase and alkali feldspar may show euhedral faces suggesting their crystallization in melt (Vernon, 1986). Biotite and sillimanite commonly occur as inclusions in cordierite, which is always a minor phase, but neither in cordierite nor in the melanosome are biotite and sillimanite in contact with each other. Most samples contain either sillimanite or biotite. These relationships suggest biotite–sillimanite consuming melting reactions forming the leucosome of the migmatites. Garnet is commonly present and almost always associated with the leucosome. Poikilitic cores containing quartz and feldspar, and in places sillimanite and biotite, might have grown in the solid state at the upper end of the prograde P–T path. The rim zones are largely inclusion free. Euhedral faces are rare; typically, the garnet shape is irregular. Crystals may reach up to 4 mm in size. The rim zones of garnet

are in textural equilibrium with leucosome phases and are likely to have formed as a cotectic phase during biotite and sillimanite breakdown. Spinel–quartz associations and pseudomorphs after osumilite, as described in Bial et al. (2015a), are also present in the Koenap Formation close to the Polisiehoek and Swartoup plutons. Samples described by Bial et al. (2015a) show similar features and assemblages, and we consider their P–T–t paths applicable to the Koenap Formation in the study area.

The Bysteek Formation contains three prominent rock types: metabasite, calc-silicate rocks, and marbles (**Figures 3B,D**). Metabasites are typically massive and fine- to medium-grained, but layered in some places. Leucosome veins are rare, and, where present, they are typically folded. The mineral assemblage is typically simple, showing clinopyroxene and anorthitic plagioclase. Ca-rich garnet is present in places. Biotite and orthopyroxene are rare, and accessories are titanite and apatite. Leucosome veins are less than 1 cm thick and contain plagioclase, minor alkali feldspar, and quartz. The melt forming reaction is unclear, but the presence of alkali feldspar suggests biotite breakdown. The melanosome seams contain clinopyroxene. The mineral assemblage of the metabasites and the presence of leucosome veins are consistent with the ultrahigh-temperature P–T conditions of the regional metamorphism (Bial et al., 2015a).

Calc-silicates are light brown fine-grained and plagioclase–quartz–dominated rocks that may contain alkali feldspar, clinopyroxene, garnet, and titanite. In addition, Moen and Toogood (2007) describe green amphibole, scapolite, and epidote, which have not been found in the current study. In places, the calc-silicate rocks contain minor calcite. The calc-silicate rocks form centimeter to several meters thick layers, interlayered with marble. Where marble and calc-silicate rocks are thinly (~<dm scale) interlayered, convoluted folding is common, and boudinage may contort the layering to form calc-silicate nodules and lenses in a marble matrix (**Figure 3D**).

Marble layers are commonly pure calcite but may contain accessory small (<2 mm) silicate grains, including orange grossularite, green olivine, or clinopyroxene. Epidote has been described by Moen and Toogood (2007) but has not been encountered in the current study. Two of the marble layers in the study area are up to ~10 m thick but more commonly they are thinner and interlayered and interfolded with calc-silicates.

### Contacts and Transitions

Relevant for this study are the contact relationships between 1) the supracrustal metamorphic rocks of the Koenap and Bysteek Formations with the Swartoup Pluton, 2) the Polisiehoek granite gneiss and the Swartoup Pluton, and 3) between the Polisiehoek Gneiss and the Koenap and Bysteek Formations.

Along the contact of the Koenap Formation with the Swartoup Pluton diffuse transitions between anatexites and plutonic rocks suggest the interaction of both rocks in their partially molten state. Furthermore, the presence of garnet-bearing granitoids within the Swartoup Pluton, about 3 m away from the contact, suggests the flow of garnet-bearing magma from the anatexites into the Swartoup Pluton's marginal zone. The interior of the Swartoup Pluton is typically garnet-free.

Restricted to a several meter-wide zone along the contact to the marbles and calc-silicates of the Bysteek Formation, the Swartoup Pluton shows a texturally distinctive lithological variety with large up to 2-cm–sized clinopyroxene in a white plagioclase- and alkali feldspar-rich matrix. This material, but not other Swartoup Pluton varieties, intrude the Bysteek granulitic metabasites, forming magmatic megabreccias (**Figure 3B**).

The contacts of the Polisiehoek granite gneiss with the supracrustal rocks and with the Swartoup Pluton are markedly different. This contact zone with both the migmatites of the Koenap Formation and the Bysteek Formation is commonly sheared. Where such deformation is absent, the contacts are planar or irregular, but always sharp. No megabreccias are related to the emplacement of the Polisiehoek magma. Abundant Polisiehoek granite dykes in both the Koenap Formation and the Swartoup Pluton show sharp and planar contacts. There is no evidence of metasomatic or melt interaction of Polisiehoek melt with any of its host rocks.

### Regional Shear Zones and Brittle Deformation

The Hartebees River shear zone, an up to ~400-m thick regional scale structure to the northeast (**Figure 2**), leaves the Swartoup Pluton largely unaffected, except of minor shear zones that are parallel to the HRSZ and are likely genetically related (**Figure 3F**). The Oup shear zone crosscuts the pluton at high angle (**Figure 2**) but in the study area is poorly exposed. Further north in the Twakputs gneiss, the Oup shear zone forms highly ductile mylonite zones.

Brittle faults are commonly associated with coarse-grained and often euhedral epidote and calcite mineralization, indicating the percolation of Ca-rich fluids. Pseudotachylyte is present in the regolith but has not been seen in situ. Büttner et al. (2013) describe similar faults and mineralizations in the Twakputs Gneiss north of the Hartebees River shear zone.

## Geochemistry

This chapter presents the results of the XRF major elemental and LA-ICPMS trace elemental analysis. Average compositions of the main lithological groups are provided with the full data set in the **Supplementary Material**.

Basic classification of the granitoids using major element geochemistry according to Middlemost (1994) is illustrated in **Figure 4**. The Swartoup granite samples form two clusters in the fields of granites and granodiorites, but display a scatter to lower silica and less alkaline granodiorite compositions. These variations can be explored by plotting the Swartoup samples according to their mineralogical criteria, such that the leucogranitoids with biotite as the sole mafic mineral plot within a restricted alkali content range, but with variable silica contents, falling into the fields of granite, granodiorite, and quartz monzonite. The pyroxene granitoids show a wider chemical variation, plotting from granite all the way to monzodiorite. The garnetiferous Swartoup granitoids show the least variation in this plot, consistently plotting in the granodiorite field.

The Polisiehoek granites fall into the field of granite, with a small compositional range (**Figure 4**). The Polisiehoek granite samples plot close to the high silica samples of Swartoup

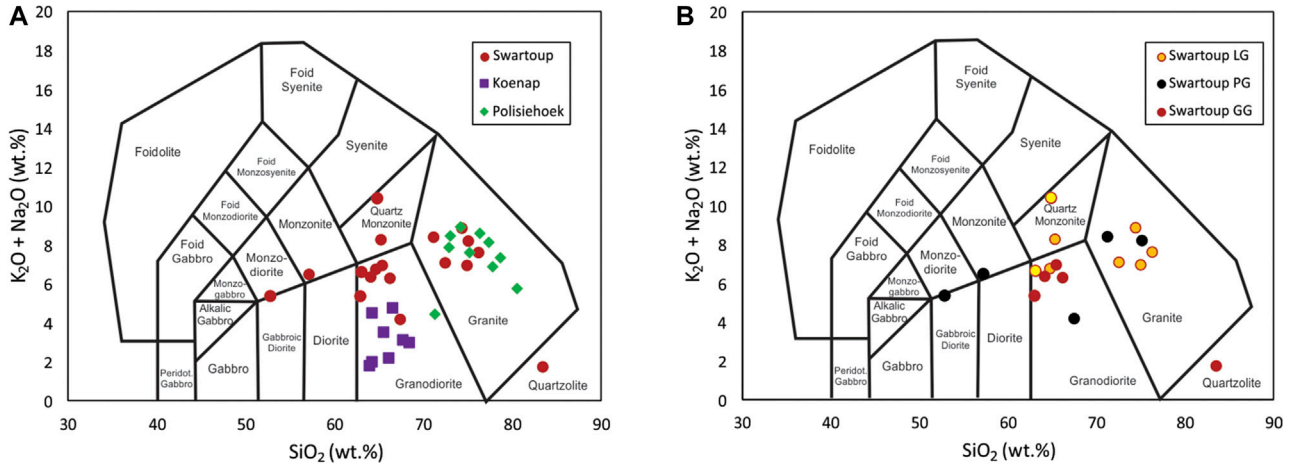


**FIGURE 4 | (A)** Total alkali vs. silica (TAS) diagram (after Middlemost, 1994) for classification of Swartoup Pluton granitoids and the Polisiehoek granite gneisses. Koenap Formation migmatites are plotted for compositional reference (as opposed to classification) purposes only. In **(B)**, the Swartoup granitoids are subdivided according to their modal compositions into leucogranitoids (LG) with biotite as the sole mafic phase, pyroxene-bearing granitoids (PG), and garnet-bearing granitoids (GG). See text for discussion.

leucogranitoids and some of the pyroxene granitoids. The Koenap migmatites and diatexites plot in the granodiorite field, with distinctly lower total alkali contents than average Polisiehoek or Swartoup plutons (**Figure 4A**). In their $SiO_2$ contents, they are similar to garnet-bearing material from the Swartoup Pluton.

## Incompatible Trace Elements

Incompatible trace elements, which can be used to illustrate genetic relationships between components potentially related by partial melting, are presented in **Figure 5**. The Swartoup granitoids are presented as the three petrologically distinguished groups (**Figures 5A–C**). Of these, the leucogranitoids and the garnet-bearing granitoids show similar trace element profiles, featuring relatively consistent patterns within the groupings, with some exceptions among the leucogranitoids. Most samples feature small negative spikes for Ba relative to Rb and Th, and show significant negative anomalies for Ta, Sr, and Ti. The garnet granitoids include samples that are distinguished from all other rocks in this study by the presence of a hump in the profile between the middle and heavy REE at the far right side of the profile, consistent with garnet accumulation in those rocks. The pyroxene granitoids are relatively heterogeneous in terms of profile patterns and element concentrations, with relatively high abundances of LILE on the left of the profile (compared to the other Swartoup groups), and samples showing either positive or negative spikes for Th, Nd, and Sm. The variation in the LREE is consistent with control by modal variation (fractionation or addition) of pyroxenes in these samples, as the main LREE-concentrating phase.

The Polisiehoek granitoids (**Figure 5D**) show large variability in some HFSE (Th, Nb, and Ta) and in Cs and Rb of one to two orders of magnitude. Sr is uniformly low, which correlates with low Ca contents in the alkali feldspar-rich and plagioclase-poor granitoid. The Koenap migmatite samples (**Figure 5E**) are characterized by uniform abundance profiles, with some variation evident in mobile large ion lithophile elements (LILE; Cs, K, and Rb, specifically).

The Bysteek Formation samples are shown for reference (**Figure 5F**). Most trace elements in the calc-silicate sample are below detection limits, while the marble shows prominent enrichment in Nb and low concentrations of LILE (including K) generally.

## REE Variations

**Figures 6A–6F** show chondrite-normalized rare-earth diagrams of the various units. The $[La/Yb]_N$ and Eu/Eu* ratios of the sample set, calculated from the data in the Supplement Material, are shown in **Table 1**.

The Swartoup leucogranitoids (**Figure 6A**) and Koenap migmatites (**Figure 6E**) show similar enrichments in REE to one another, with Ce averaging around 20–30× chondrites, and with similar magnitudes of LREE enrichment. Compared to the leucogranitoids, the HREE profiles of the migmatites (**Figure 6E**) are flat. Koenap migmatites are also characterized by distinct negative Eu anomalies, whereas Swartoup Pluton leucogranites exhibit a mixture of negative and positive Eu anomalies. The mixture of both positive and negative Eu anomalies in rocks with otherwise broadly similar REE profiles is most consistent with local redistribution of feldspar crystals in the crystallizing magma, as feldspars are the only phases which strongly concentrate Eu (as $Eu^{+2}$) relative to the other REE (Henderson, 1984). In sharp contrast, the Swartoup pyroxene granitoids (**Figure 6B**) show nonuniform REE abundances, profile slopes, and Eu anomaly size and direction, consistent with the variability displayed in their major and trace element chemistry. The garnet granitoids show distinctive patterns (**Figure 6C**), featuring enrichments in the heavy middle to heavy rare-earth elements, and distinctive depletions in the light middle rare-earth elements in two samples, with no or small negative Eu anomalies in those

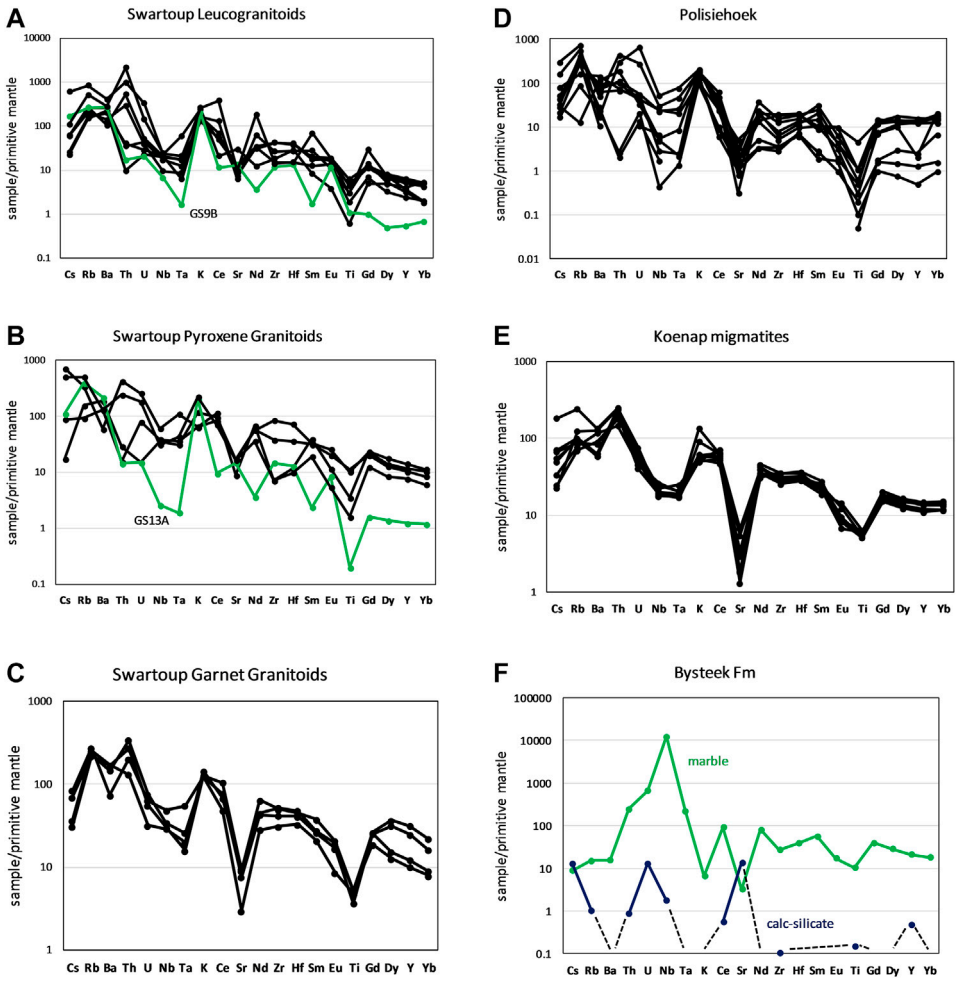


**FIGURE 5 |** Incompatible element spidergrams, normalized to Primitive Mantle (Bulk Silicate Earth pyrolite) of McDonough and Sun (1995). See text for additional information.

samples. Sample GS16A, which is from a garnet-rich quartzo-feldspathic zone, is accordingly poor in LREE with a prominent enrichment in HREE consistent with garnet accumulation.

Most Polisiehoek granitic gneisses (**Figure 6D**) have REE profiles similar to those of Koenap Formation migmatites, showing relatively uniform profiles characterized by LREE enrichment at about 100–200× chondritic values, well-defined negative Eu anomalies, and flat to gently increasing HREE profiles. The REE profile of the Bysteek Formation marble shows fairly flat LREE contents between 200× chondrite concentrations, a small negative Eu anomaly, and a shallow and uniform decline in HREE. One of the clinopyroxene-bearing Swartoup granites (**Figure 6B**) from nearby the contact to the Bysteek Formation shows a similar REE pattern.

## Radiogenic Isotopic Compositions

Sr and Nd isotopic compositions were determined for 19 granitoid samples, as well as four migmatites and one marble sample. The Rb-Sr isotopic compositional data are presented in **Table 2**, and the distributions for the granitoids are shown on a $^{87}Rb/^{86}Sr$ vs. $^{87}Sr/^{86}Sr$ isochron diagram in **Figure 7**. Some linear arrays are evident, but none of the suites can statistically be classified as isochrons based on their Model 3 solutions according to Ludwig (2012). Hence, the data are shown relative to reference lines with the corresponding ages and initial $^{87}Sr/^{86}Sr$ ratios (labeled as R*i*) indicated for each unit.

The Rb–Sr isotopic compositions show a set of subparallel aligned arrays defined by samples from the Koenap Formation migmatites, the Polisiehoek granitoids, and most of the Swartoup granitoids, corresponding to slope ages of around 1,200 Ma. The Koenap Formation data correspond to a slope age of ~1,200 Ma (**Figure 7B**) albeit with a regression imprecision of ±150 Ma and an MSWD of 41. The Sr initial isotope ratio is 0.716 ± 8. The Polisiehoek sample set shows a wide range in Rb/Sr ratio attributable to the highly variable Rb concentrations, which range from 51 to 423 ppm (**Table 2**), whereas Sr shows a restricted concentration range (32–81 ppm). The Swartoup Pluton samples show a high variability, with the leucogranitoid samples aligned along a linear trend consistent with their expected age of ~1,200 Ma.

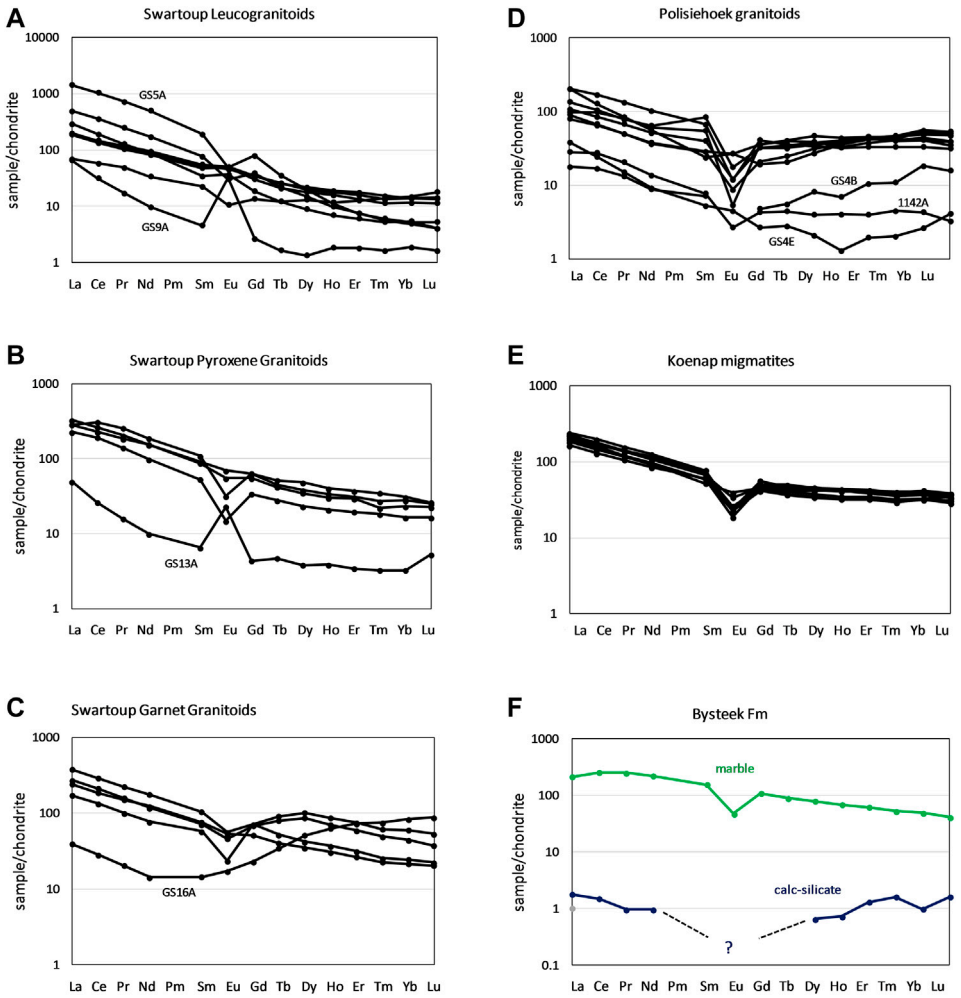


**FIGURE 6 |** Chondrite-normalized rare-earth diagrams of the Swartoup and Polisiehoek plutons and their host rocks. Compositionally distinct samples are labeled and/or distinguished using color.

The Sm–Nd isotopic compositions (**Figure 8**; **Table 3**) contrast with the Rb–Sr isotopic dataset, inasmuch as the Sm–Nd data show linear arrays constrained between reference lines corresponding to ages of ~900 Ma and around 760 Ma. Five Swartoup granitoids and all four Polisiehoek granitoid samples lie near the 900 Ma reference line. The Koenap Formation migmatites and many of the Swartoup leucogranitoids lie near the 760 Ma reference line. Neither of these trends bears any close relationship to a slope derived from the intrusion age at ~1,200 Ma.

## DISCUSSION

In its exposed shape, the Swartoup pluton forms a small body amongst significantly larger younger plutons, such as the ~1,203 Ma Polisiehoek or ~1,101 Ma Naros plutons (Pettersson, 2008; Bial et al., 2015b). It was emplaced as a layer not more than a few hundred meters thick. Dykes of the Polisiehoek pluton cut the Swartoup Pluton (**Figure 3C**) and the UHT metamorphic supracrustal migmatites and granulites of the Koenap and Bysteek Formations along sharp intrusive contacts. By contrast, the contacts between the Swartoup Pluton and the migmatites of the Koenap Formation are transitional or gradational in places where they were not affected by the tectonic overprint. Garnet-rich patches with gradational boundaries to Swartoup leucogranites likely formed from proximal Koenap Formation magma injections, and may be present several meters within the Swartoup Pluton. This indicates the emplacement of the Swartoup Pluton during the presence of melt in the Koenap Formation. The main phase of anatexis has been dated as ~1,225–1,175 Ma, with the highest temperature (spinel–quartz and osumilite stability) reached early in this time interval (Bial et al., 2015a). The emplacement of the Swartoup magma into (ultra-) hot crust is also indicated by the transitional contacts of mafic Bysteek Formation granulites and intruding melt (**Figure 3B**).

**TABLE 1 |** $[La/Yb]_N$ ratios and Eu*/Eu ratios.

| Rock type | Sample | $[La/Yb]_N$ | Eu*/Eu | Rock type | Sample | $[La/Yb]_N$ | Eu*/Eu |
|---|---|---|---|---|---|---|---|
| Swartoup Leucogran | GS5A | 86.90 | 1.91 | Koenap migmatite | 1137A | 5.99 | 1.70 |
| | GS9A | 5.03 | 1.74 | | 1138A | 4.22 | 2.44 |
| | GS9B | 40.40 | 0.11 | | 1141A | 4.93 | 2.89 |
| | GS15B | 2.80 | 2.70 | | 1143A | 7.46 | 2.23 |
| | 1144A | 12.90 | 0.97 | | 1143B | 6.79 | 2.21 |
| | 1145A | 14.70 | 0.88 | | 1147B | 6.80 | 1.72 |
| | 1146A | 16.30 | 0.81 | | GS4C | 5.93 | 2.80 |
| | 1149A | 54.60 | 0.72 | | GS4D | 5.92 | 1.24 |
| Swartoup Px Gran | GS10B | 15.00 | 1.30 | | | | |
| | GS11D | 8.14 | 2.72 | Polisiehoek Granitoid | 1136A | 3.29 | 2.12 |
| | GS13A | 15.10 | 0.24 | | 1142A | 6.33 | 2.24 |
| | GS13B | 12.50 | 2.92 | | 1147C | 6.12 | 4.56 |
| Swartoup Gt Gran | 1139A | 14.80 | 1.55 | | 1148A | 1.87 | 2.81 |
| | 1140A | 10.70 | 1.20 | | 1148B | 2.35 | 2.99 |
| | GS7A | 5.50 | 1.51 | | 1152A | 4.40 | 0.80 |
| | GS15C | 235 | 2.73 | | GS1A | 2.30 | 1.19 |
| | GS16A | 0.53 | 1.57 | | GS4B | 1.62 | — |
| Bysteek | GS10A | 4.02 | 2.77 | | GS4E | 18.90 | 0.90 |
| Fm | GS19A | 1.12 | — | | GS11B | 2.42 | 8.59 |

*Eu*/Eu is defined as $[(0.5\times(Sm + Gd))/Eu]_N$. Samples GS19A (Bysteek marble specimen) and GS4B (Polisiehoek granite gneiss) contain no detectable Eu. Samples were normalized to CI carbonaceous chondrite of McDonough and Sun (1995).*

The significantly larger Polisiehoek pluton was emplaced after the migmatites and the Swartoup Pluton solidified, but prior to cooling to low temperature. Folds related to the formation of the Swartoup antiform, and the mylonite zones parallel to the Hartebees and Oup shear zones in both plutons and the supracrustal host rocks formed above the stability of white mica or other phases indicating temperatures of the mid-amphibolite facies or lower. Bial et al. (2015b), Bial et al. (2016) propose the formation of first-order structures in the Kakamas Domain at about 1,120–1,130 Ma, which is in agreement with the 1,101 ± 6 Ma Naros Pluton truncating the Hartebees River shear zone and large-scale fold structures (Bial et al., 2015b). All these suggest slow cooling of the crust after the regional metamorphic peak.

These field relations, with evident interaction between the Swartoup magma and the melt in the hosting Koenap migmatites and the Bysteek mafic/calcic granulites, bear the potential of a local origin of the Swartoup Pluton. The diatectic Koenap Formation forms a large outcrop in the region (**Figures 1**, **2**), and may well have generated a several hundred-meter-thick granitic pluton. The much larger Polisiehoek granite gneiss was emplaced at a later time, and no field observation indicates any direct (i.e., transitional) relationship between the granite and its host rocks. In the following sections, we assess the potential sources of both the Swartoup and Polisiehoek plutons and the possible contributions of the Koenap and Bysteek Formations to their composition.

## Radiogenic Isotopic Constraints on Granitoid Source Rocks

The radioisotopic compositional variation can provide first-order estimates on timing and contributions from various prospective chemical reservoirs. **Figure 9** shows the distribution of the granitoid rocks in $\varepsilon_{Nd}{}^{1200\ Ma}$ vs. $^{87}Sr/^{86}Sr^{1200\ Ma}$ space, as well as the Koenap migmatites, relative to Bulk Earth, the Depleted Mantle, and approximated Kakamas Domain area crustal reservoir. Isotopic compositions have been calculated for 1,200 Ma, based on the existing age of ~1,203 Ma for the Polisiehoek intrusion, and an estimated age of ~1,215–1,225 Ma for the Koenap migmatite.

The least variable data, the Koenap migmatite samples, plot with a restricted range of Nd and Sr isotopic compositions, which is consistent with their derivation from melting of Mesoproterozoic crust (**Figures 9A,B**). While a, at the time, very young crust (~1.3 Ga) would not have evolved enough by 1.2 Ga to account for the Koenap Formation data, contributions from older crustal material, such as a mixture of ~1.6 and 1.3 Ga crust, would be appropriate. Equally possible is a mixture of 1.3 Ga crust with a small contribution from ~2.4 Ga crust, as invoked by Eglington (2006) and Bailie et al. (2017) as the preferred crustal contamination end-member for granitoids in the central Namaqua Sector. Abundant inherited zircon of Paleoproterozoic (1.8–2.1 Ga) and early Mesoproterozoic (1.4–1.6 Ga) ages in granites and migmatites in the region (Bial et al., 2015a; Bial et al., 2015b) support the presence of such sources in the Kakamas Domain.

The Swartoup leucogranitoids and garnet granitoids (LG, GG in **Figure 9**) plot as distinctly less evolved compositions than the Koenap Formation, and therefore these Swartoup granitoids cannot represent a pure (closed system) partial melt of the Koenap migmatite. These samples overlap directly with the least-radiogenic samples from the coeval to slightly younger Keimoes Suite in the eastern Kakamas Domain (**Figure 9A**; Bailie et al., 2017) and the southern Bushmanland Domain (Bailie et al., 2019). They are consistent with derivation from a mixture of Koenap Formation and a juvenile depleted mantle-

**TABLE 2 |** Radiogenic isotopic data for this study. (Rb–Sr isotopic compositional data).

| Rock type | Sample | Rb (ppm) | Sr (ppm) | $^{87}Rb/^{86}Sr$ | $^{87}Sr/^{86}Sr$ | ±2σ | $^{87}Sr/^{86}Sr$ at 1200 Ma |
|---|---|---|---|---|---|---|---|
| Koenap migmatite | 1137A | 74.26 | 135.17 | 1.5490 | 0.74403 | 15 | 0.71785 |
| | 1138A | 41.85 | 37.84 | 3.1183 | 0.76847 | 20 | 0.71575 |
| | 1143B | 56.24 | 68.20 | 2.3248 | 0.75723 | 9 | 0.71792 |
| | 1147B | 146.06 | 66.64 | 6.1801 | 0.82536 | 11 | 0.72088 |
| Bysteek marble | GS19A | 0.62 | 271.90 | 0.0064 | 0.70660 | 10 | 0.70649 |
| Swartoup Leucogran. | GS5A | 161.20 | 124.10 | 3.7817 | 0.76766 | 13 | 0.70373 |
| | GS9A | 499.20 | 588.85 | 2.4627 | 0.74523 | 12 | 0.70360 |
| | GS9B | 156.50 | 261.00 | 1.7399 | 0.73342 | 13 | 0.70401 |
| | GS15B | 311.10 | 195.25 | 4.6468 | 0.78548 | 11 | 0.70693 |
| | 1145A | 88.39 | 263.75 | 0.9715 | 0.72345 | 13 | 0.70703 |
| | 1146A | 157.46 | 248.65 | 1.8381 | 0.73661 | 15 | 0.70554 |
| | 1149A | 124.28 | 146.64 | 2.4624 | 0.74727 | 14 | 0.70564 |
| Swartoup Px Gran. | 1151A | 55.51 | 339.36 | 0.4738 | 0.71459 | 13 | 0.70658 |
| | GS11D | 204.65 | 175.20 | 3.3972 | 0.75712 | 11 | 0.69969 |
| | GS10B | 93.50 | 337.80 | 0.8015 | 0.71245 | 13 | 0.69890 |
| Swartoup Gt Gran. | GS13A | 236.70 | 291.05 | 2.3625 | 0.74540 | 11 | 0.70546 |
| | GS13B | 304.60 | 323.40 | 2.7372 | 0.74952 | 10 | 0.70325 |
| | GS7A | 137.55 | 150.65 | 2.6553 | 0.75649 | 10 | 0.71160 |
| Polisiehoek granite gneiss | 1136A | 131.18 | 81.31 | 4.7136 | 0.80462 | 14 | 0.72494 |
| | 1142A | 51.06 | 34.53 | 4.3129 | 0.78507 | 24 | 0.71215 |
| | 1148A | 216.99 | 30.71 | 21.202 | 1.08293 | 41 | 0.72451 |
| | 1152A | 171.20 | 65.15 | 7.7135 | 0.85279 | 25 | 0.72239 |
| | GS1A | 94.15 | 100.05 | 2.7376 | 0.75988 | 10 | 0.71360 |
| | GS11B | 423.20 | 31.75 | 40.866 | 1.31344 | 16 | 0.62259 |

*Rb/Sr calculated from Sr and Rb concentrations determined by LA-ICP-MS on fused beads. See Analytical Methods section for further details.*

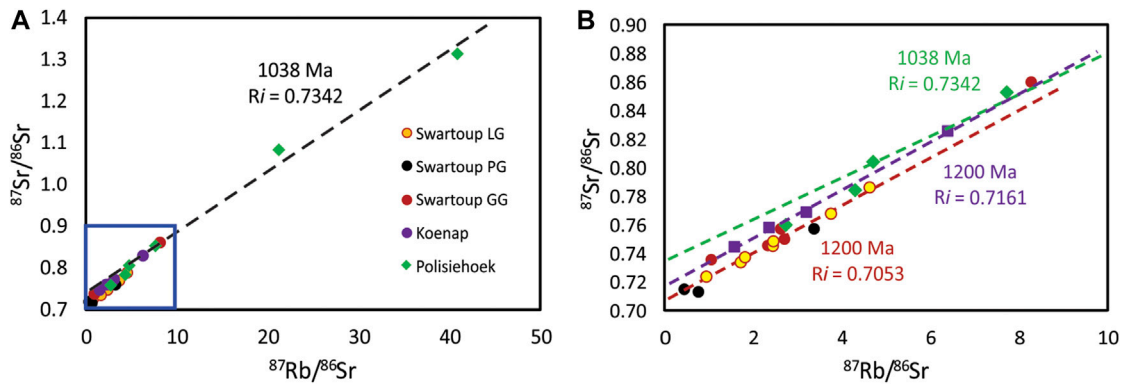


**FIGURE 7 |** Rb–Sr isochron diagram for the granitoids. **(A)** All samples from the Polisiehoek granite gneiss, extending to high Rb/Sr ratios in a near-linear array. The lower left of the diagram containing the Swartoup Pluton and Koenap Fm. samples is expanded in **(B)**, showing the linear arrays with best-fit reference lines, with age and initial $^{87}Sr/^{86}Sr$ ratios shown corresponding to their slope. The reference line for the Swartoup pluton is based on five samples only. See text for discussion. Swartoup LG, PG, and GG = leucogranitoid, pyroxene granitoid, and garnet granitoid, respectively.

derived melt (**Figure 9B**), or alternatively with the remelting of a source which contained a mixture of juvenile crust and older granitoid crust.

The observed initial $^{87}Sr/^{86}Sr$ ratios for the Swartoup pyroxene granitoids and Polisiehoek granitoids (**Figure 9A**) show a wide range in initial ratio, but are largely consistent with the compositional range reported by Bailie et al. (2017) and Bailie et al. (2019), both in terms of anomalously radiogenic and anomalously (improbably) unradiogenic compositions. This range in $^{87}Sr/^{86}Sr$ values from ~Bulk Earth (or lower) to ~0.77 is not correlated to complementary $\varepsilon_{Nd}^{1200}$ compositional variation. It cannot be readily attributable to bulk crustal contamination based on the compositional range of the known reservoirs, and is therefore most readily attributable to post-crystallizational mobility of Rb in these rocks. This is consistent with the evidence for LILE enrichment shown in the incompatible trace element spidergrams for the Swartoup pyroxene granitoids and the Polisiehoek granitoids (**Figures 5B,D**). The related implications will be discussed in more detail below.

Based on initial $^{87}Sr/^{86}Sr$ and $\varepsilon_{Nd}^{1200}$, a juvenile mantle melt contribution cannot be excluded as the least-radiogenic end-member, but it is not required to explain the data. The effect of the variable Rb-Sr systematics can be eliminated by plotting the chondrite-normalized $^{147}Sm/^{144}Nd$ ratio ($f_{Sm/Nd}$) against $\varepsilon_{Nd}^{1200}$.

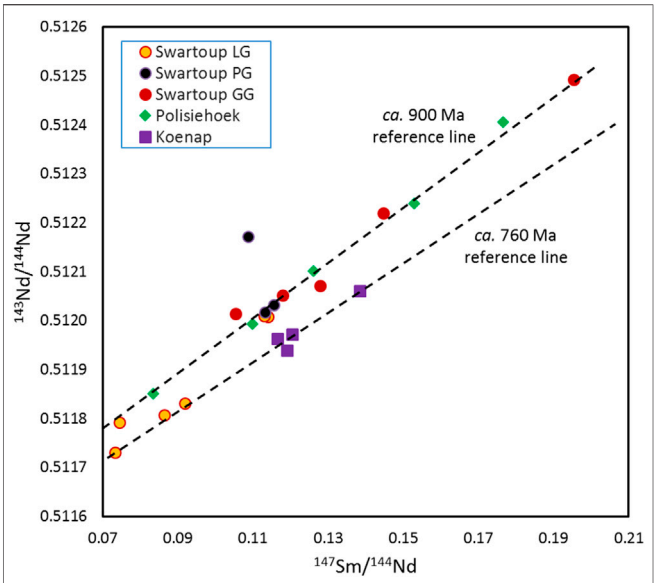


**FIGURE 8 |** Sm–Nd "isochron" diagram for the Swartoup Hills granitoid suite. See text for details.

**Figure 10** shows the dataset from this study in the context of the data range of local crust (Yuhara et al., 2002; Eglington, 2006; Pettersson et al., 2009; Bailie et al., 2017). Based on this diagram, the Kakamas Domain granitoid compositions potentially could be derived from three contributing components. 1) A mantle-derived partial melt, originating between around 1.6 to 1.5 Ga (i.e., Mesoproterozoic isotopically enriched mantle-derived partial melt); 2) LREE-enriched rocks which are slightly (perhaps 100–200 million years) older than the intrusions; and 3) much older, early Paleoproterozoic crust. Key points here include the following:

(1) A juvenile partial melt of an isotopically enriched mantle could explain end-member 1, or a mafic crust significantly older than the formation of the granites. Constraints on the possible involvement of an enriched mantle source will be discussed further below. Note that, critically, the depleted mantle end-member (end-member 1 in **Figure 10**) cannot be a juvenile (i.e., ~1,200 Ma) melt derived from partial melting of the depleted mantle asthenosphere; the $\varepsilon_{Nd}{}^{1200\ Ma}$ vs. $^{87}Sr/^{86}Sr^{1200\ Ma}$ plot in **Figure 9** is deceiving in this context, as the isotopically depleted component is not, in fact, the LREE-depleted component.
(2) The isotopically depleted but LREE-enriched end-member (end-member 2 in **Figure 10**) is strongly represented in multiple data sets (Bailie et al., 2017; this study), in the Swartoup Hills most prominently reflected in the Polisiehoek granitoid dataset, which displays a linear mixing line.
(3) Minimal contribution from much older crust (end-member 3 in **Figure 10**) is required to explain the composition of granitoids in the Swartoup Hills.

Late Paleoproterozoic (~2.4–2.2 Ga) crustal rocks have been invoked to explain local isotopic compositions (Eglington, 2006; Bailie et al., 2017; 2019), and as modeled in **Figure 9** for the Namaqua Metamorphic Complex data of Yuhara et al. (2002), which lie comfortably along a Paleoproterozoic mixing curve in **Figure 9A**. However, still older crustal rocks, such as potentially

**TABLE 3 |** Radiogenic isotopic for the Swartoup Hills. (Sm–Nd isotopic compositional data).

| Rock type | Sample | Nd (ppm) | Sm (ppm) | $^{143}Nd/^{144}Nd$ | 2σ | $^{147}Sm/^{144}Nd$ | $\varepsilon_{Nd}$, at 1200 Ma |
|---|---|---|---|---|---|---|---|
| Koenap migmatite | 1137A | 49.8 | 9.96 | 0.511972 | 12 | 0.1204 | −1.3 |
| | 1138A | 38.6 | 8.86 | 0.512061 | 14 | 0.1383 | −2.3 |
| | 1143B | 44.3 | 8.57 | 0.511962 | 17 | 0.1164 | −0.9 |
| | 1147B | 49.8 | 9.84 | 0.511940 | 15 | 0.1190 | −1.7 |
| Swartoup Leucogran. | GS5A | 80.4 | 15.3 | 0.511807 | 28 | 0.1145 | −3.6 |
| | GS9B | 40.4 | 7.81 | 0.511831 | 22 | 0.1163 | −3.4 |
| | GS15B | 37.7 | 7.08 | 0.511731 | 21 | 0.1130 | −4.8 |
| | 1145A | 42.9 | 8.11 | 0.512007 | 10 | 0.1139 | +0.4 |
| | 1146A | 37.7 | 7.08 | 0.512101 | 11 | 0.1130 | +0.6 |
| | 1149A | 40.8 | 5.05 | .0511792 | 9 | 0.0744 | +2.3 |
| | 1151A | 70.0 | 13.5 | 0.512032 | 14 | 0.1156 | +0.6 |
| Swartoup Px Gran. | GS11D | 85.1 | 16.0 | 0.512017 | 22 | 0.1131 | +0.7 |
| | GS10B | 42.9 | 8.11 | 0.512171 | 13 | 0.1139 | +3.6 |
| Swartoup Ga Gran. | GS13A | 4.52 | 0.96 | 0.512071 | 15 | 0.1279 | −0.5 |
| | GS13B | 44.5 | 7.77 | 0.512015 | 17 | 0.1052 | +1.9 |
| | GS15C | 35.3 | 8.47 | 0.512219 | 15 | 0.1446 | −0.2 |
| | GS16A | 6.56 | 2.13 | 0.512492 | 19 | 0.1953 | −2.6 |
| | GS7A | 53.4 | 10.5 | 0.512052 | 17 | 0.1178 | +0.7 |
| Polisiehoek granite gneiss | 1136A | 16.5 | 4.20 | 0.512101 | 11 | 0.1260 | +0.4 |
| | 1142A | 25.4 | 3.52 | 0.511993 | 16 | 0.1099 | +0.8 |
| | 1148A | 27.8 | 8.15 | 0.512239 | 16 | 0.1530 | −1.1 |
| | 1152A | 6.25 | 2.33 | 0.511851 | 23 | 0.0833 | +2.1 |
| | GS1A | 17.3 | 4.22 | 0.512182 | 15 | 0.1466 | −1.2 |
| | GS11B | 40.8 | 5.05 | 0.512405 | 12 | 0.1765 | −1.5 |

*Sm/Nd calculated from Sm and Nd concentrations determined by LA-ICP-MS on fused beads. See Methodology section for further details.*

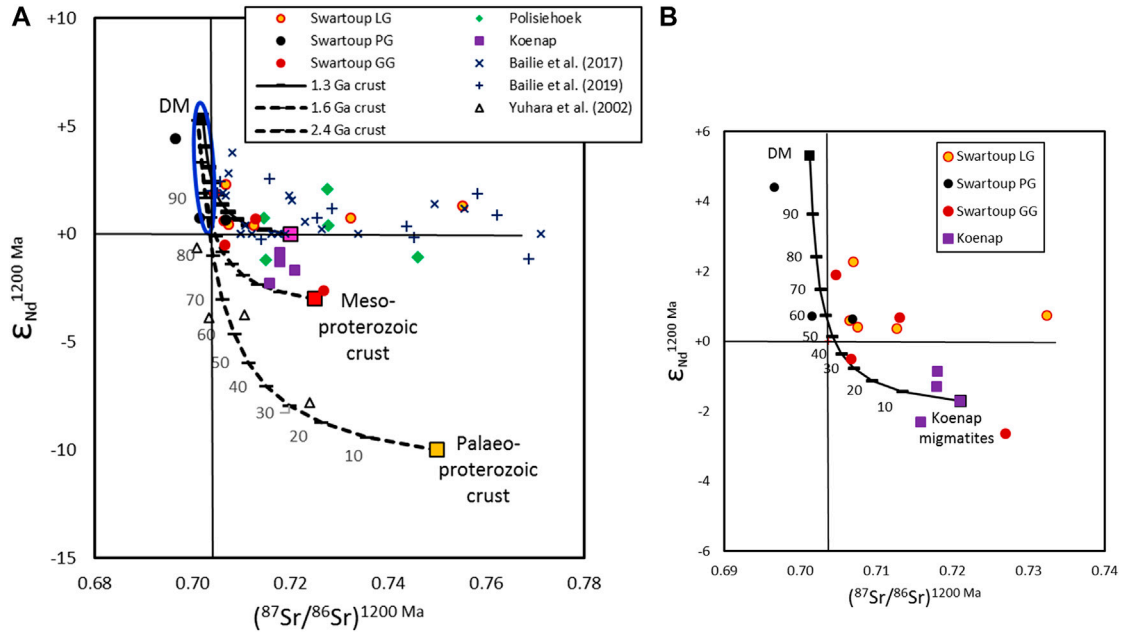


**FIGURE 9 |** Initial Sr and Nd isotopic compositions, corrected to 1,200 Ma, the approximate age of the Polisiehoek granite emplacement. Bulk Earth composition indicated by black lines. **(A)** Approximate positions for the depleted mantle (DM, in the blue ellipse), and Mesoproterozoic (1.3 Ga, magenta square; 1.6 Ga red square) and Paleoproterozoic (1.9 Ga; orange square) crustal rocks. Mixing models corresponding to addition of a mantle-derived end-member to crustal reservoirs of ~1.3, 1.6, and a 2.4 Ga ages are indicated by the graduated curves. In **(B)**, the mixing of Koenap sample 1147B, compositions with depleted mantle is modeled with reference to the Swartoup granitoid samples. Data for Bulk Earth from McCulloch and Wasserburg (1978), depleted mantle from DePaolo (1981) and Faure (1986) for Nd and Sr, respectively. Regional crustal reservoir compositions are based on Namaqua Province datasets from Yuhara et al. (2002), Eglington (2006), and Bailie et al. (2017) for combined Sm–Nd and Rb–Sr data, Sm–Nd data from Pettersson et al. (2009), and Rb–Sr from Clifford et al. (1975). See text for additional details.

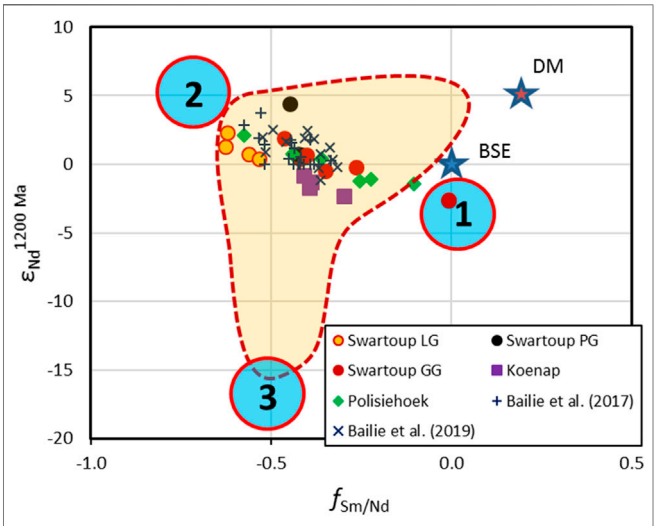


**FIGURE 10 |** Chondrite-normalized Sm/Nd ratio ($f_{Sm/Nd}$) plotted against $\varepsilon_{Nd}^{1200}$. Pale orange field with dashed border: Namaquan crust based on Yuhara et al. (2002), Eglington (2006) and Pettersson et al. (2009). DM, depleted mantle; BSE, bulk silicate Earth, as represented here by the Chondritic Uniform Reservoir (CHUR) composition to which the plot is normalized. The three blue circles indicate the minimum number and suggested compositional characteristics of end-members required to explain the distribution of data for the Swartoup Hills granitoids. See text for discussion.

recycled late Archaean rocks, are required in order to accommodate $\varepsilon_{Nd}^{1200\ Ma}$ values < −15, as reported (and so interpreted) by Pettersson et al. (2009). However, for the Swartoup Hills (this study), Keimoes Suite (Bailie et al., 2017), and Kliprand Dome (Bailie et al., 2019) datasets, there is minimal, if any, contribution of this older crust evident. However, the presence of a Paleoproterozoic heritage in the crust of the Kakamas Domain in general, as indicated by abundant $T_{DM}$ data (Pettersson et al., 2009) and by inherited zircon, is not disputed.

## Derivation of the LREE-Enriched Non-radiogenic Nd Component

A source region capable of generating melts with LREE enrichment and isotopically depleted Nd (positive $\varepsilon_{Nd}^{1200\ Ma}$) is typically one involving a significant component of partial melt derived from a juvenile depleted mantle. Given that according to DePaolo (1981) depleted mantle has a composition around $\varepsilon_{Nd}^{1200\ Ma}$ = +5.2, and the most depleted samples from this study are between +1.9 and +3.6, there is some allowance for a small amount of mixing between a mantle source and existing crust. Bailie et al. (2017) reported two samples from the nearby Keimoes Suite with similarly isotopically depleted Nd ($\varepsilon_{Nd}^{1200\ Ma}$ of +2.8 to +3.8) and low Sm/Nd ($^{147}Sm/^{144}Nd < 0.095$).

Depleted mantle signatures are associated with A-type ("anorogenic") granites and form from a combination of

differentiated basaltic melts and/or remelted quartzo-feldspathic crust (Eby, 1992; Whalen et al., 1996; Frost and Frost, 2011). Such melts are only moderately and locally modified by metasomatism or crystal fractionation. A-type melts occur worldwide throughout geological time in a variety of tectonic settings and do not necessarily indicate an anorogenic or rifting environment. In the Namaqua Sector, coeval flood basalts (or voluminous mafic dyke swarms or any other component of a Large Igneous Province) are entirely absent, arguing against an M-type (mantle-derived; Eby, 1992) differentiate origin. By contrast, the abundant zircon formation around ~1.3 Ga in the central Namaqua Sector provides evidence for the presence of slightly older high-grade metamorphic basement rocks. An unspecified modified (by virtue of having non–mantle-like Sr isotopic compositions) A-type granite source is therefore proposed as the compositional end-member 2 of **Figure 10**.

## Alkali Metasomatism

Samples of the Polisiehoek and the Swartoup pyroxene granitoids, as well as most of the Keimoes Suite of Bailie et al. (2017) and the Kliprand Dome (Bailie et al., 2019) datasets, display prominent age-corrected $^{87}Sr/^{86}Sr$ enrichment (**Figure 9A**). The effects of alkali enrichment can be illustrated in a plot of Rb against Sr, a less mobile alkaline earth element (in aqueous solutions), in **Figure 11A**. For reference to an even less mobile element, Rb variation with the high field strength element (HFSE) Nd is also shown (**Figure 11B**). In both plots, enrichment in Rb evident in samples of Polisiehoek and the Swartoup pyroxene granitoids is not correlated to increases in the HFSE.

The lack of correlation between LILE and HFSE enrichment means that the enrichment process could involve an aqueous solution in which the LILE are soluble but not the HFSE, as distinct from a partial melt, where both chemical groups would be expected to be mobilized equally. In **Figure 11A**, the enrichment in Rb for (some) samples of the Polisiehoek and Swartoup pyroxene granitoids, as well as numerous samples from the Keimos and Kliprand suites, with over 200 ppm Rb, are contrasted with the Swartoup leucogranites, garnet granitoids, and the Koenap migmatites, all of which show relatively restricted variation in Rb and in Sr, suggesting less secondary Rb enrichment.

The LREE enrichment evident in **Figure 10** is evidently not a consequence of LREE enrichment in absolute terms. **Figure 11B** shows that the samples that show Rb enrichment are typically those low in Nd. This process is thus not linked to bulk crustal contamination by radiogenic older crust, for example, where enrichment in Rb and LREE would be correlated with increased $^{87}Sr/^{86}Sr$ and increasingly negative $\varepsilon_{Nd}{}^{1200}$ values. The LILE enrichment evident in the spidergrams for the Polisiehoek granite gneiss (**Figure 5D**) and Swartoup pyroxene granitoids (**Figure 5B**) is therefore interpreted as a response to alkali metasomatism, through which Rb (along with other alkali and mobile alkaline earth elements) was introduced as a post-magmatic open system event, thereby interfering with the Rb–Sr systematics of those samples. The samples featuring the highest Rb concentrations also have very high measured $^{87}Sr/^{86}Sr$, indicating that the metasomatic process probably occurred not long after crystallization, rather than in recent times, where the Rb enrichment would not be supported by any additional radiogenic Sr accumulation. Nonetheless, back-calculation of $^{87}Sr/^{86}Sr$ for these samples shows both anomalously low or high values at 1,200 Ma, consistent with an artifact of age correction based on modified Rb/Sr ratios.

There are a number of potential events following granite emplacement which represent possible fluid metasomatic episodes. During the prolonged and slow cooling of the crust after the ~1,200 Ma thermal peak, secondary monazite in metapelitic host rocks formed at ~1,090–1,070 Ma, possibly related to fluid mobility and a late heating event during the ~1,100 Ma Naros Pluton emplacement (Bial et al., 2015a). At ~1,000 Ma, the emplacement of the late-Mesoproterozoic pegmatite belt in the Namaqua Sector was a further episode that may have caused widespread fluid mobility in the crust (Bial et al., 2015a; Doggart, 2019). Such pegmatites are abundant in the study area. Furthermore, during the waning stages of the Neoproterozoic Pan-African orogeny, the area was affected by brittle faulting and foreland seismicity, leading to the formation of pseudotachylyte (~512 Ma) and epidote mineralization along faults (Büttner et al., 2013), features that are also present in the Swartoup Pluton. However, in the absence of petrographic evidence for a pervasive low-temperature hydrothermal event, our preference from these options would be to attribute the alkali metasomatism to fluid activity in the ~100 million years following Swartoup granite emplacement, associated with prolonged elevated temperatures.

The Rb enrichment in the Polisiehoek and some of the Keimoes samples corresponding to an Rb/Sr ratio around 10 is not correlated to Sr enrichment, so is not obviously explained by metasomatism or contamination related to carbonate supracrustal rocks, which suggests that two separate processes are required to explain the alkali enrichment and the Ca enrichment. However, Marcantonio et al. (1990) modeled between 10 and 30% contamination of their granites by host-rock marble, which was manifested as distinctively heavy $\delta^{18}O$ values (~+10), but was not evident in Sr or Nd isotopic compositions nor in Ca enrichments. They note that effective modeling of this is made more uncertain by the generally low REE concentrations and heterogeneous isotopic compositions of the marbles. They suggested that this apparent contradiction could perhaps be accounted for by fluid metasomatism involving $CO_2$-rich fluids in the granite source area, rather than by bulk marble assimilation during emplacement. This explanation could allow that both the alkali enrichment and the Ca enrichment events could be attributed to carbonate contamination, in the form of separate geochemically distinct processes. A regional fluid metasomatism may explain the alkali enrichment, which locally takes place in combination with physical assimilation effects explaining the bulk contamination. The data of Marcantonio et al. (1990) do not show any of the characteristic heterogeneity in initial $^{87}Sr/^{86}Sr$ ratio which features in this study and those of Bailie et al. (2017, 2019), nor is their fluid contamination event specifically characterized by alkali enrichment. On these grounds, two distinct contamination processes are indicated for the Swartoup and Polisiehoek plutons.

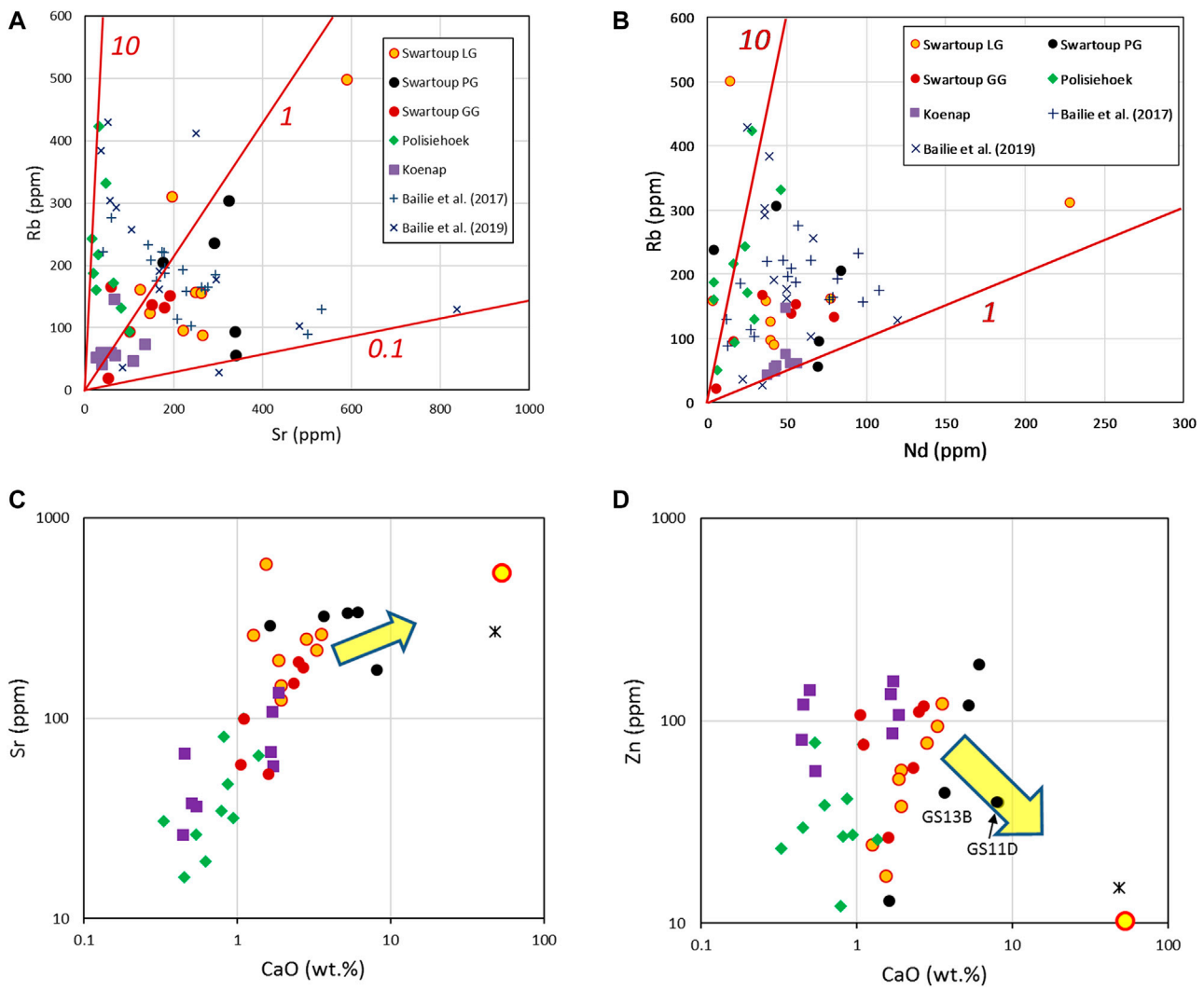


**FIGURE 11 |** Variation of Rb vs. **(A)** Rb vs. Sr and **(B)** Rb vs. Nd, for the Swartoup Hills granitoids and migmatite, as well as the granitoids of Bailie et al. (2017) and Bailie et al. (2019). Lines of constant Rb/Sr or Rb/Nd ratio are shown in red, with values indicated. In **(C)** CaO vs Sr and **(D)** CaO vs. Zn data are plotted, with reference to a sample of the Bysteek Formation marble (plotted as an asterisk) and average back-arc limestones (yellow symbol; Zhang et al., 2017). The arrows indicate direction of mixing from an average Swartoup granitoid toward the carbonate compositions.

## Carbonate Contamination

The Rb enrichment in the pyroxene granitoids and some of the Keimoes and Kliprand rocks shown in **Figure 11A** do show correlated increases in Rb and Sr along trends corresponding to Rb/Sr ratios of around 1 and 0.1. These latter trends could be linked to the effects of syn-emplacement carbonate (marble or calc-silicate) assimilation or fluid mobilization processes, as manifested in the petrology of some of the Swartoup pyroxene granitoids. The marbles of the Bysteek Formation in the immediate vicinity of the Swartoup pluton provide the obvious source for this process.

Geochemically, the trace element compositions of the granitoids are not prominently influenced by elemental enrichments or depletions typically related to carbonates, as noted in the text accompanying **Figures 5**, **6**, except that the REE profiles for Swartoup pyroxene granitoid samples GS-13B, and in particular GS-11D, are virtually identical in both profile shape and elemental abundances to the Bysteek marble profile in **Figure 8F**. Samples GS-11D and -13B were collected from nearby the pluton contact to the Bysteek Formation (**Figure 2**).

Geochemical evidence for local contributions from the marbles to the Swartoup granitoids can be seen more clearly in plots of CaO against Sr and Zn (**Figures 11C,D**). The compositional trends here suggest that only a few samples of pyroxene granitoid, collected in sight of the Bysteek Formation calcic and carbonate rocks, actually reflect direct compelling chemical evidence for carbonate contamination.

## Incompatible Trace Element Constraints on Granitoid Source Rocks

Given the demonstrated open system behavior in the alkali and alkaline earth metals, and the potential effects of carbonates,

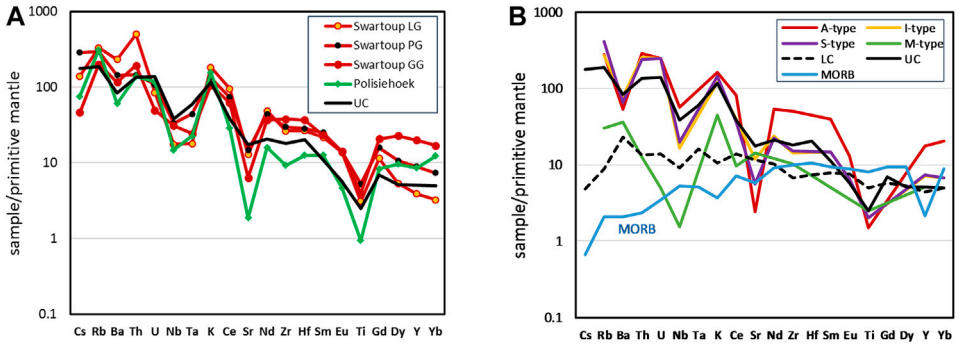


**FIGURE 12 |** Primitive mantle-normalized trace element spidergrams. **(A)** Average Swartoup Hills granitoid compositions (this study), and **(B)** I-, S-, M-, and A-type granites from Whalen et al. (1987) and Collins et al. (1982). Reference compositions of Upper and Lower Crust and average MORB from Taylor and McLennan (1995).

classification diagrams based on major element oxide ratios are probably not reliable as petrogenetic indicators for these intrusions in this setting. The trace element distribution patterns (including both LILE and HFSE; **Figure 12**) of Swartoup Hills granitoids can, however, usefully be compared to those of granitoids from subduction settings (Whalen et al., 1987) and intraplate A-type settings (Collins et al., 1982; Whalen et al., 1987). The trace element profiles for S- (sedimentary rock protolith) and I- (igneous origins) type granites are similar to one another, with the most pronounced distinction being the more prominent negative Sr anomaly for I-type granitoids. Contrastingly, the A-type (anorogenic, within-plate) granitoids feature a significantly larger negative Sr anomaly than the other types, and significant relative enrichment in REE and Zr. Bial et al. (2015b) interpreted the characteristics of the Schuitdrift granite gneiss (**Figure 1B**), a hornblende-biotite mesocratic granitoid, as the product of fractional crystallization from a mafic mantle-derived source melt. These rocks show relative enrichment in Th, high REE, modest relative depletions in Nb and Ti, and a strong negative anomaly for Sr. In contrast, the associated leuco-granitoid rocks show prominent negative anomalies for Nb and Ti, and were interpreted as the products of partial melting of sedimentary protoliths with no mantle-derived melt contributions.

In this context, all of the granitoids analyzed in this study show some affinities to the A-type profile, specifically with regard to the high Th/U ratios, prominent negative anomalies for Sr, and high REE contents (**Figures 12A,B**). The absence of a prominent Zr depletion in the Swartoup granitoids is also consistent with the A-type granitoid profile. However, the Nb anomaly of the rocks in this study is comparable to that typical of I- and S-type granitoids, and is significantly smaller than that observed in the leucogranitic paragneisses further north described by Bial et al. (2015b). This combination of diagnostic features is therefore consistent with the mixed protolith origins that have been proposed, such that neither a purely anorogenic-type protolith nor a metasedimentary one is appropriate for any of these intrusions. The Polisiehoek granite gneiss (**Figure 12B**), which shows the most prominent negative Ba, Nb, and Sr anomalies, but almost MORB-like REE and Zr, perhaps best exemplifies this mix of diagnostic features. Because this geochemical pattern represents a heavily modified A-type granite signature, it cannot easily be accommodated directly into the compositional subclassifications of A-type granites. None of the Swartoup Hills samples actually plot convincingly within the A-type granite fields of Eby (1992), or within the ferroan granite fields of Frost and Frost (2011). However, their Y/Nb ratios are all >1, with elevated Rb/Nb and Sc/Nb ratios, more consistent with A-type granites derived from I-type protoliths ($A_2$ granites of Eby, 1992), rather than as mantle melt fractionation products ($A_1$ granites of Eby, 1992). According to the alternative classification scheme of Frost and Frost (2011), the Polisiehoek granite samples largely qualify as ferroan, consistent with the siliceous members of other A-type granites. By contrast, the Swartoup and Polisiehoek samples are modified to varying extents toward more calcic and calc-alkalic compositions. Given that the correlation of A-type granite geochemistry with specific petrogenetic and tectonic settings is problematic at best (Whalen et al., 1996), an origin involving a mixture of crustal- and mantle-derived sources appears to be the most defensible interpretation for A-type granites broadly, with the Swartoup and Polisiehoek plutons showing much stronger affiliations to remelted granitic crust rather than to basaltic differentiates.

## Heterogeneity of Granitoid Source Rocks in the Namaqua Sector

Neodymium isotope diagrams for different domains and sub-domains in the Namaqua Sector (**Figure 13**) suggest that different compositional reservoirs were accessed to different extents in different places. The ages of granitoid emplacement, between ~1,230 and 950 Ma (Thomas et al., 1994, 2016; Macey et al., 2015), are broadly consistent across the Namaqua Sector, so no temporal evolution of sources is indicated from these data. Five potential source components are identified here, characterized as follows:

(1) Depleted mantle; characterized by positive values of $\varepsilon_{Nd}^{1200\ Ma}$, unradiogenic $^{87}Sr/^{86}Sr$, and LREE-depletion relative to HREE.

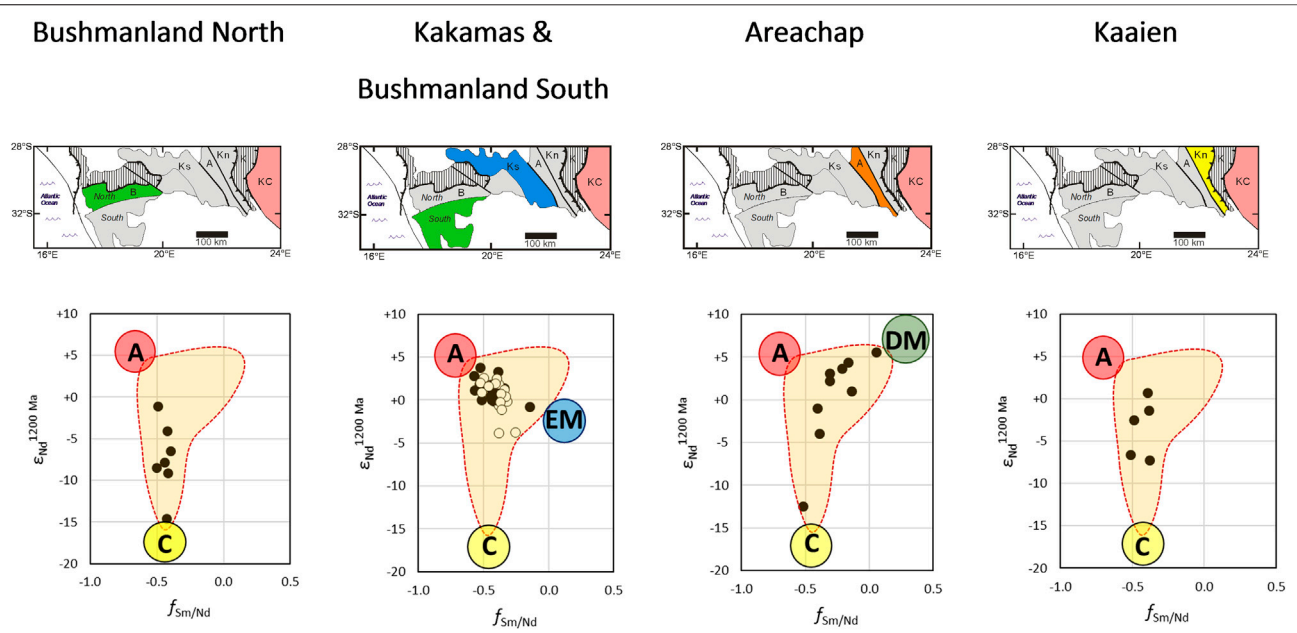


**FIGURE 13 |** Source variation with geographic position and different domains. Bushmanland North data from Yuhara et al. (2002) and Pettersson et al. (2009); Bushmanland South data from Yuhara et al. (2002), Pettersson et al. (2009), and Bailie et al. (2019); Kakamas (Ks) data from Bailie et al. (2017) and this study; Areachap and Kaaien data from Pettersson et al. (2009). B, Bushmanland; Ks, Kakamas; A, Areachap; Kn, Kaaien; K, Kheis; KC, Kaapvaal Craton. Vertically-lined fields are 2.4–2.2 Ga pre-Namaquan regions (see also **Figure 1**). Granite magma sources: A, anorogenic granite source; C, Paleo-/Mesoproterozoic crust; EM, enriched mantle; DM, depleted mantle.

(2) Mesoproterozoic mafic magma, which has the characteristics of an enriched mantle; weakly negative values of $\varepsilon_{Nd}^{1200\ Ma}$, moderately enriched $^{87}Sr/^{86}Sr$, and LREE-depletion relative to HREE (end-member 1 in **Figure 10**).
(3) Anorogenic granite source, characterized by positive values of $\varepsilon_{Nd}^{1200\ Ma}$, unradiogenic $^{87}Sr/^{86}Sr$, and LREE enrichment relative to HREE (end-member 2 in **Figure 10**).
(4) Mesoproterozoic felsic crust, with $\varepsilon_{Nd}^{1200\ Ma}$ of ~-5 to -10, radiogenic $^{87}Sr/^{86}Sr$, and LREE enrichment relative to HREE (end-member 3 in **Figure 10**, which has been separated into younger and older Proterozoic crust here).
(5) Paleoproterozoic felsic crust, with $\varepsilon_{Nd}^{1200\ Ma}$ of ~−15 to −20, radiogenic $^{87}Sr/^{86}Sr$, and LREE enrichment relative to HREE.

## Bushmanland North

The northern Bushmanland Domain is proximal to the Paleoproterozoic Richtersveld Domain and contains a significant proportion of Paleoproterozoic rocks, such as the Steinkopf gneiss and the Gladkop Suite (Nke et al., 2020). According to Bailie et al. (2019), the proportion of Mesoproterozoic crust formation decreases from the south to the north in the Bushmanland Domain. The spread of $\varepsilon_{Nd}^{1200\ Ma}$ between ~0 and −15 indicates mixing between relatively old crustal source and an anorogenic granite source. The older components are likely Paleoproterozoic rocks similar to those in the Richtersveld Domain, for which Pettersson et al. (2009) report $\varepsilon_{Nd}^{1200\ Ma}$ of −13. There is no evidence for the involvement of any mafic, LREE-depleted crust, or mantle sources. We may tentatively conclude that the source rocks for these granitoids consisted mainly of felsic crustal rocks only, with no juvenile or older mafic sources providing significant contributions.

## Kakamas and Bushmanland South

The Kakamas Domain, where the largest dataset is available, shows a strong clustering adjacent to the anorogenic granite source (**Figure 13**), with a significant contribution (more evident in **Figure 10**) from an enriched mafic mantle source. These data are consistent with the partial melting of a granulitic lower crust, forming the A-type component, and the addition of coeval juvenile isotopically enriched mafic mantle magmas. Significant early Mesoproterozoic (~1.5 Ga) or Paleoproterozoic crustal sources are not required to explain the data distribution in the Kakamas or southern Bushmanland Domains.

## Areachap

In their $\varepsilon_{Nd}^{1200\ Ma}$ and $f_{Sm/Nd}$ patterns, the data from the Areachap Domain (**Figure 13**), approaching the Kaapvaal Craton, overlap with those from the adjacent Kakamas Domain, but in addition some data points support the involvement of a depleted mantle source, combining mainly with Mesoproterozoic felsic crust. Arguably, the anorogenic granite source is represented here as well. A few of the samples from the Keimoes granitoid suite of Bailey et al. (2017), plotted here as part of the Kakamas Domain, actually lie within the Areachap Domain, and strongly show the influence of the A-type source here as well. There are no compositional

distinctions evident between samples from either side of the domain boundary. One sample, collected from the interior of the domain, just south of the town of Upington (Pettersson et al., 2009), has an $\varepsilon_{Nd}^{1200\ Ma}$ of −12.5, which requires the involvement of a significantly older crustal source, probably representing the Paleoproterozoic heritage indicated for the entire Namaqua Sector by $T_{DM}$ and zircon ages. In this domain, the source rocks incorporated a significant component of juvenile mantle melt, along with older felsic crust. This would be consistent with the interpretations of Pettersson et al. (2009), who note the distinctive presence in this domain of arc-related supracrustal sequences without mature metasediments, and a provenance combining juvenile and older rocks.

## Kaaien

The few data available from the Kaaien Domain, close to the Paleoproterozoic rocks of the Kheis Subprovince, show a pattern similar to those of the northern Bushmanland Domain, which is also adjacent to a Paleoproterozoic domain. The data show the involvement of early Mesoproterozoic crust and the anorogenic granite source, with no requirement for early Paleoproterozoic crust nor any LREE-depleted mafic source.

What stands out as broad observations from these data sets is that there is no clear geographical trend of increasing or decreasing involvement of any one source component, such as might be anticipated from west to east with increasing proximity to the Kaapvaal Craton. Interpretations of this type are restricted by the fact that magmatic rocks of different ages in a dynamic tectonic evolution are combined within the data sets. The northern Bushmanland Domain shows prominent involvement of older crust, consistent with its proximity to the Richtersveld Domain immediately to the north, as noted by Bailie et al. (2019) and Nke et al. (2020). However, the data currently available from domains which parallel the Archean Kaapvaal Craton boundary to the east show no such systematic affinities to old source rocks. However, without more extensive data, this cannot be meaningfully assessed.

## Source Heterogeneity in Granitoids of the Namaqua Sector

The processes and sources of granitoids in the Swartoup Hills reflect the larger scale processes active in other domains in the Namaqua Sector. The dominant magma sources are, with variable proportions, an A-type granite source, a mafic magma contribution generated from an isotopically enriched source, and magma generated form early Mesoproterozoic or Paleoproterozoic crust. The isotopic characteristics of the A-type component indicate that the source rocks were not significantly older (e.g., early Meso- or Paleoproterozoic) than the age of their partial melting event. Bial et al. (2015a) report magmatic zircon of ~1,300–1,350 Ma in metapelites from the Swartoup Hills, attributed to a high-temperature metamorphic stage predating the ~1,200 Ma episode of crustal anatexis. Similar ages are reported for volcanic rocks in the Areachap Domain (~1,275–1,371 Ma; Pettersson et al., 2007; Bailie et al., 2010), for orthogneiss slices along the Lower Fish River Onseepkans Thrust Zone (1,320–1,270 Ma; Macey et al., 2016), and for the Konkiep Domain in central Namibia (1,330–1,380 Ma; Hoal and Heaman, 1995; Becker, 2008; Cornell et al., 2015), indicating the large scale of intense heat influx into the continental crust at that time. Potentially, the source of the A-type granite component formed at that time.

Isotopically, the mafic melt component could have formed either from crust that had formed several hundred million years prior to its partial melting, or from a juvenile partial melt from an enriched mantle source. There is no evidence in the Namaqua Sector of abundant presence of mafic crust, neither of Mesoproterozoic nor Paleoproterozoic age. By contrast, mafic plutonism and volcanism across the Namaqua Sector and during several episodes of the crustal evolution indicate mantle melting. For example, the Jerusalem gabbronorite (**Figure 1B**), in nearby southernmost Namibia, intruded the crust of the Kakamas Domain at the same time as the bulk of the granitic plutons (pers. commun. Paul Macey, 2020). Abundant partial melting of an enriched asthenospheric mantle and the effective mixing of such melts with coeval felsic lower crustal melts are possible, and likely to occur, in a continental back-arc setting (Bial et al., 2015a; Büttner, 2020), where hot crust is underlain by thin lithospheric mantle, and partial asthenospheric mantle melting is common, particularly during extensional episodes. Conversely, neither terrane accretion or continent–continent collisions, nor volcanic arcs, provide such a setting, as they both typically display thickened crust and lithosphere, and do not support the long-standing high-temperature/low-pressure regime that is observed in the Namaqua Sector (Büttner, 2020).

Granitoids with $\varepsilon_{Nd}$ signatures indicating early Mesoproterozoic or Paleoproterozoic crustal sources are unproblematic to explain in the Namaqua Sector. U-Pb ages of inherited zircon components of such age and $T_{DM}$ ages spreading from ~1.4 to 2.4 Ga (e.g., Eglington, 2006; Pettersson et al., 2007, 2009; Bial et al., 2015a,b; Macey et al., 2015) testify to the presence of rocks of this age and active crust forming processes at that time.

## Granite Emplacement in the Swartoup Hills

The Swartoup granitoid and Polisiehoek granite plutons in the Kakamas Domain were emplaced into host rocks of variably metapelitic, calc-silicate, mafic and carbonatic compositions during a high-temperature orogenic episode. Along its margin, the Swartoup Pluton shows significant contamination by its host rocks. Contamination by calcic host rocks of the Bysteek Formation formed macroscopically conspicuous features such as the growth of millimeter- to centimeter-sized clinopyroxene. This is consistent with geochemical evidence for localized carbonate contamination of the granitoid. The Polisiehoek pluton, although significantly larger than the Swartoup Pluton, and therefore arguably with a higher potential to interact with its host rocks, does not show evidence of significant chemical or physical interaction with its host rocks during its emplacement. Although the crust at that time of emplacement was still at granulite facies conditions, intrusive contacts are sharp. The Polisiehoek magma, without contribution of melt contamination from its host rocks, was generated in deeper

crustal and mantle levels. We attribute the more intense contamination of the Swartoup Pluton magma by its host rocks to the magma emplacement at the regional ultrahigh temperature metamorphic peak with abundant anatectic melt present in the host rock, temperatures that allowed even the mafic granulites of the Bysteek Formation to react with the intruding granitic melt. Conversely, the larger Polisiehoek granite was much more pervasively affected by alkali metasomatism that resulted in significant mobility of Rb and heterogeneous apparent initial $^{87}Sr/^{86}Sr$ as a result.

## SUMMARY AND CONCLUSIONS

The Swartoup Hills granitoid suite and associated migmatites, as a component of the Kakamas Domain, show the following characteristics:

The Swartoup granites, granodiorites, and quartz monzonites intruded the felsic migmatitic gneisses of the Koenap Formation and marbles and calc-silicates of the associated Bysteek Formation. Radiogenic isotopic evidence requires that the Swartoup Pluton rocks could not have been derived solely by partial melting of the Koenap Formation metapelites. The main source material for the Swartoup Pluton is geochemically and isotopically consistent with an A-type granitic source, mixed with an isotopically enriched LREE-depleted, and hence mantle-derived contribution. The variable composition of the Swartoup granitoids seems to imply composite pluton characteristics. However, contamination from the proximal supracrustal Bysteek Formation carbonates, forming clinopyroxene granitoids, or the presence of garnet, possibly entrained in melt injections from nearby Koenap Formation migmatites, are restricted to narrow marginal zones. We attribute these contaminations to the emplacement of the Swartoup Pluton during the regional metamorphic peak, with the associated anatectic melt mobility and high reactivity of the host rocks. The narrow shape of the layer forming the Swartoup Pluton, causing a high surface/volume ratio, likely promoted the proportional abundance of magma contamination from the host rocks.

The Polisiehoek granites, which have intruded the Swartoup granitoids, were derived from a mixture of the A-type granite source and a larger component of the enriched mantle source. They show no evidence of contamination from their host rocks, which is in agreement with the sharp intrusive contacts to all other rock types. This indicates that at the time of pluton emplacement, most likely around 1,203 Ma (Pettersson et al., 2009), the Swartoup Pluton, and the Koenap Formation migmatites had solidified. Neither the Swartoup nor the Polisiehoek granitoids require the contribution of significantly older crustal (i.e., early Meso- or Paleoproterozoic) material in their sources.

The Polisiehoek granites and some Swartoup leucogranitoids have been strongly but heterogeneously affected by alkali metasomatism that is not obviously linked to carbonate assimilation or metasomatism, but which cannot be eliminated as a possible source of $CO_2$-rich alkaline aqueous fluids. This has significantly influenced the Rb–Sr isotope systematics in the Kakamas Domain. This is also evident in the Keimoes Suite rocks further to the east, as well as in the southern Bushmanland Domain, but is not evident in any of the Koenap Formation migmatite samples from the Swartoup Hills. Repeated heating and/or magma emplacement between ~1,100 and ~1,000 Ma, or Pan-African fault bound fluid influx may explain possible fluid sources, although the absence of a hydrothermal mineralogical overprint suggests that this metasomatism occurred as a late-magmatic high temperature process, rather than in association with a discrete lower temperature hydrothermal process.

The main magma sources of plutons in the Swartoup Hills, comprising a mantle magma generated by partial melting of enriched subcontinental asthenosphere, and an A-type magma generated from Mesoproterozoic crust, are compatible with the sources of granitoids across the entire Namaqua Sector. The consistency of magma sources for granitic plutons across the Namaqua Sector suggests a uniform tectonic setting across the belt, in which Mesoproterozoic crust generates partial melt at times when also fertile mantle sources and conditions are present to contribute melt that is blended with the crustal melts in the lower crust. The longevity of plutonism in the Namaqua Sector between ~1,300 and ~1,000 Ma points to a tectonic setting in which the main magma sources remain regionally available, and in which the required high temperatures were maintained or regenerated over long periods in relatively thin lithosphere. A mobile continental back-arc appears to be the only setting in which this is possible.

## DATA AVAILABILITY STATEMENT

The original contributions presented in the study are included in the article/**Supplementary Material**, and further inquiries can be directed to the corresponding author.

## AUTHOR CONTRIBUTIONS

SB: Geological context and introduction, field mapping and field relationships, sample collection, petrography, discussion and interpretations. SP: Geochemical and isotope data processing, data documentation, interpretation and writeup, petrological model of magma evolution, discussion and interpretation. GS: Fieldwork, sample collection, some petrography and data processing, parts of the Analytical Methods section.

## ACKNOWLEDGMENTS

Constructive reviews by G Shellnut, K-N Pang and J Dostal are gratefully acknowledged for improvements to the manuscript. Fieldwork and analytical costs for this project were supported *via* Rhodes University RC Grants to SB.

## SUPPLEMENTARY MATERIAL

The Supplementary Material for this article can be found online at: https://www.frontiersin.org/articles/10.3389/feart.2020.602870/full#supplementary-material.

## REFERENCES


Abrahams, Y., and Macey, P. H. (2020). Lithostratigraphy of the Mesoproterozoic Donkieboud granodiorite (Komsberg Suite), South Africa and Namibia. *S. Afr. J. Geol.* 123, 421–430. doi:10.25131/sajg.123.0028

Bailie, R., Abrahams, G., Bokana, R., van Bever-Donker, J., Frei, D., and Le Roux, P. (2019). The geochemistry and geochronology of the upper granulite facies Kliprand Dome: comparison of the southern and northern parts of the Bushmanland Domain of the Namaqua Metamorphic Province, southern Africa and clues to its evolution. *Precam. Res.* 330, 58–100. doi:10.1016/j.precamres.2019.04.011

Bailie, R., Gutzmer, J., and Rajesh, H. (2010). Lithogeochemistry as a tracer of the tectonic setting, lateral integrity and mineralization of a highly metamorphosed Mesoproterozoic volcanic arc sequence on the eastern margin of the Namaqua Province, South Africa. *Lithos* 119, 345–362.

Bailie, R., Macey, P. H., Nethenzheni, S., Frei, D., and le Roux, P. (2017). The Keimoes Suite redefined: the geochronological and geochemical characteristics of the ferroan granites of the eastern Namaqua Sector, Mesoproterozoic Namaqua-Natal Metamorphic Province, southern Africa. *J. Afr. Earth Sci.* 134, 737–765. doi:10.1016/j.jafrearsci.2017.07.017

Bailie, R., Rajesh, H. M., and Gutzmer, J. (2012). Bimodal volcanism at the western margin of the Kaapvaal Craton in the aftermath of collisional events during the Namaqua-Natal Orogeny: the Koras Group, South Africa. *Precam. Res.* 200-203, 163–183. doi:10.1016/j.precamres.2012.01.017

Baxter, S., and Feely, M. (2002). Magma mixing and mingling textures in granitoids: examples from the Galway Granite, Connemara, Ireland. *Mineral. Petrol.* 76, 63–74. doi:10.1007/s007100200032

Becker, T. (2008). "The Kairab Formation east of Sesriem and the associated subvolcanic intrusive rocks." In *The geology of Namibia*., Editor R. M. G. Miller (Windhoek, Namibia: Geological Survey), Vol. 2, 8-10–8-16.

Bial, J., Büttner, S. H., and Appel, P. (2016). Timing and conditions of regional metamorphism and crustal shearing in the granulite facies basement of south Namibia: implications for the crustal evolution of the Namaqualand metamorphic basement in the Mesoproterozoic. *J. Afr. Earth Sci.* 123, 145–176. doi:10.1016/j.jafrearsci.2016.07.011

Bial, J., Büttner, S. H., and Frei, D. (2015b). Formation and emplacement of two contrasting late-Mesoproterozoic magma types in the central Namaqua Metamorphic Complex (South Africa, Namibia): evidence from geochemistry and geochronology. *Lithos* 224–225, 272–294. doi:10.1016/j.lithos.2015.02.021

Bial, J., Büttner, S. H., Schenk, V., and Appel, P. (2015a). The long-term high-temperature history of the central Namaqua Metamorphic Complex: evidence for a Mesoproterozoic continental back-arc in southern Africa. *Precam. Res.* 268, 243–278. doi:10.1016/j.precamres.2015.07.012

Büttner, S. H. (2020). Comment on "Evidence for Mesoproterozoic collision, deep burial and rapid exhumation of garbenschiefer in the Namaqua front, South Africa" by Valby Van Schijndel, David H. Cornell, Robert Anczkiewicz, Anders Schersten, Geoscience Frontiers, Volume 11, Issue 2, Pages 511–531. *Geosci. Front.* 11, 1889–1894. doi:10.1016/j.gsf.2020.04.007

Büttner, S. H., Fryer, L., Lodge, J., Diale, T., Kazondunge, R., and Macey, P. (2013). Controls of host rock mineralogy and $H_2O$ content on the nature of pseudotachylyte melts: evidence from Pan-African faulting in the foreland of the Gariep Belt, South Africa. *Tectonophys* 608, 552–575. doi:10.1016/j.tecto.2013.08.024

Chappell, B. W., White, A. J. R., Williams, I. S., and Wyborn, D. (2004). Low- and high-temperature granites. *Earth Sci.* 95, 125–140. doi:10.1017/S0263593300000973

Clarke, D. B. (1992). *Granitoid rocks*. London, UK: Chapman & Hall.

Clemens, J. D., Holloway, J. R., and White, A. J. R. (1986). Origin of an A-type granite: experimental constraints. *Am. Mineral.* 71, 317–324.

Clemens, J. D. (2003). S-Type granitic magmas – petrogenetic issues, models and evidence. *Earth-Sci. Rev.* 61, 1–18. doi:10.1016/S0012-8252(02)00107-1

Clemens, J. D., and Stevens, G. (2012). What controls chemical variation in granitic magmas. *Lithos* 134-135, 317–329. doi:10.1016/j.lithos.2012.01.001

Clemens, J. D., and Vielzeuf, D. (1987). Constraints on melting and magma production in the crust. *Earth and Planet. Sci. Letters* 86, 287–306. doi:10.1016/0012-821X(87)90227-5

Clifford, T. N., Barton, E. S., Retief, E. A., Rex, D. C., and Fanning, C. M. (1995). A crustal progenitor for the intrusive anorthosite–charnockite kindred of the cupriferous Koperberg Suite, O'okiep district, Namaqualand, South Africa; new isotope data for the country rocks and the intrusives. *J. Petrol.* 36, 231–258. doi:10.1093/petrology/36.1.231

Clifford, T. N., Barton, E. S., Stern, R. A., and Duchesne, J.-C. (2004). U-Pb zircon calendar for Namaquan (Grenville) crustal events in the granulite-facies terrane of the O'okiep Copper District of South Africa. *J. Petrol.* 45, 669–691. doi:10.1093/petrology/egg097

Clifford, T. N., Gronow, J., Rex, D. C., and Burger, A. J. (1975). Geochronological and petrogenetic studies of high-grade metamorphic rocks and intrusives in Namaqualand, South Africa. *J. Pet.* 16, 154–188. doi:10.1093/petrology/16.1.154

Collins, W. J., Beams, S. D., White, A. J. R., and Chappell, B. W. (1982). Nature and origin of A-type granites with particular reference to southeastern Australia. *Contrib. Mineral. Petrol.* 80, 189–200. doi:10.1007/BF00374895

Colliston, W. P., Cornell, D. H., Schoch, A. E., and Praekelt, H. E. (2015). Geochronological constraints on the Hartbees River Thrust and Augrabies Nappe: new insights into the assembly of the Mesoproterozoic Namaqua-Natal Province of southern Africa. *Precambr. Res.* 265, 150–165. doi:10.1016/j.precamres.2015.03.008

Cornell, D. H., Pettersson, Å., Whitehouse, M. J., and Scherstén, A. (2009). A new chronostratigraphic paradigm for the age and tectonic history of the Mesoproterozoic Bushmanland Ore District, South Africa. *Econ. Geol.* 104, 1277–1281. doi:10.2113/gsecongeo.104.8.1277

Cornell, D. H., van Schijndel, V., Simonsen, S. L., and Frei, D. (2015). Geochronology of Mesoproterozoic hybrid intrusions in the Konkiep terrane, Namibia, from passive to active continental margin in the Namaqua-Natal Wilson Cycle. *Precambr. Res.* 265, 166–188. doi:10.1016/j.precamres.2014.11.028

DePaolo, D. J. (1981). Neodymium isotopes in the Colorado Front Range and crust–mantle evolution in the Proterozoic. *Nature* 291, 193–196. doi:10.1038/291193a0

Diener, J. F. A., White, R. W., Link, K., Dreyer, T. S., and Moodley, A. (2013). Clockwise, low-P metamorphism of the Aus granulite terrain, southern Namibia, during the Mesoproterozoic Namaqua Orogeny. *Precam. Res.* 224, 629–652. doi:10.1016/j.precamres.2012.11.009

Doggart, S. (2019). Geochronology and isotopic characterisation of LCT pegmatites from the Orange River Pegmatite Province. MSc thesis, Stellenbosch, South Africa: Stellenbosch University, 234.

Eby, G. N. (1992). Chemical subdivision of the A-type granitoids: petrogenetic and tectonic implications. *Geology* 20, 641–644. doi:10.1130/0091-7613(1992)020<0641:CSOTAT>2.3.CO

Eglington, B. M. (2006). Evolution of the Namaqua-Natal Belt, southern Africa – a geochronological and isotope geochemical review. *J. Afr. Earth Sci.* 46, 93–111. doi:10.1016/j.jafrearsci.2006.01.014

Faure, G. (1986). *Principles of isotope geology*. 2nd Edition, Hoboken, NJ: John Wiley & Sons, Inc. 588 pp.

Frost, C. D., and Frost, B. R. (2011). On ferroan (A-type) granitoids: their compositional variability and modes of origin. *J. Pet.* 52, 39–53.

Groenewald, C. A., and Macey, P. A. (2020). Lithostratigraphy of the Mesoproterozoic Yas-Schuitdrift Batholith, South Africa and Namibia. *S. Afr. J. Geol.* 123, 431–440. doi:10.25131/sajg.123.0029

Harris, C., Le Roux, P., Cochrane, R., Martin, L., Duncan, A.R., Marsh, J.S., Le Roex, A.P., and Class, C. (2015). The oxygen isotope composition of Karoo and Etendeka picrites: High δ18O mantle or crustal contamination? Contrib. Mineral. Petrol. 170, 8, doi:10.1007/s00410-015-1164-1

Henderson, P. (1984). "General geochemical properties and abundances of the rare earth elements", in *Rare earth element geochemistry*., Editor P. Henderson (Amsterdam, Netherlands: Elsevier Science Publishers B. V.), 1–32.

Hoal, B. G., and Heaman, L. M. (1995). The Sinclair sequence: U–Pb age constraints from the Awasib Mountain area. *Commun. Geol. Surv. Namib.* 10, 83–91.

Joubert, P. (1986). Namaqualand - a model of Proterozoic accretion? *Transact. Geol. Soc. South Africa.* 89, 79–96.

King, P. L., White, A. J. R., Chappel, B. W., and Allen, C. M. (1997). Characterization and origin of aluminous A-type granites from the Lachland Fold Belt, southeastern Australia. *J. Pet.* 38, 371–391. doi:10.1093/petroj/38.3.371

Ludwig, K. R. (2012). *User's manual for Isoplot 3.75: a geochronological toolkit for Microsoft Excel*. Berkeley, CA: Berkeley Geochronology Center, Special Publication No. 5.

Ma, J.-L., Wei, G.-J., Liu, Y., Ren, Z.-Y., Xu, Y.-G., and Yang, Y.-H. (2013). Precise measurement of stable ($\delta^{88/86}$Sr) and radiogenic ($^{87}$Sr/$^{86}$Sr) strontium isotope

ratios in geological standard reference materials using MC-ICP-MS. *Chin. Sci. Bull.* 58, 3111–3118. doi:10.1007/s11434-013-5803-5

Macey, P. H., Lambert, C. W., Kisters, A. F. M., Gresse, P. G., Thomas, R., Miller, J. A., et al. (2016). *Towards a new geodynamic model for the western Namaqua Province*. Cape Town, South Africa: 35th International Geological Congress.

Macey, P. H., Minnaar, H., Miller, J. A., Lambert, C., Kisters, A. F. M., Diener, J., et al. (2015). *The Precambrian geology of the Warmbad region, southern Namibia. An interim explanation to 1:50 000 geological map sheets of the 1: 250 000 2818 Warmbad sheet*. Geological Survey of Namibia and Council for Geoscience of South Africa, Windhoek, Pretoria.

Macey, P. H., Thomas, R. J., Minnaar, H. M., Gresse, P. G., Lambert, C. W., Groenewald, C. A., et al. (2017). Origin and evolution of the ~1.9 Ga Richtersveld Magmatic Arc, SW Africa. *Precam. Res.* 292, 417–451. doi:10.1016/j.precamres.2017.01.013

Marcantonio, F., McNutt, R. H., Dickin, A. P., and Heaman, L. M. (1990). Isotopic evidence for the crustal evolution of the frontenac arch in the Grenville Province of Ontario, Canada. *Chem. Geol.* 83, 297–314. doi:10.1016/0009-2541(90)90286-G

McCulloch, M. T., and Wasserburg, G. J. (1978). Sm-Nd and Rb-Sr chronology of continental crust formation. *Science* 200, 1003–1011. doi:10.1126/science.200.4345.1003

McDonough, W. F., and Sun, S.-S. (1995). The composition of the Earth. *Chem. Geol.* 120, 223–253. doi:10.1016/0009-2541(94)00140-4

Middlemost, E. A. K. (1994). Naming materials in the magma/igneous rock system. *Earth Sci. Rev.* 37, 215–224. doi:10.1016/0012-8252(94)90029-9

Miller, R. Mc. G. (2008). *The geology of Namibia*. Vol. 1. *Archaean to Mesoproterozoic. Minestry of Mines and Energy*., Geological Survey, Windhoek.

Miller, R. McG. (2012). Review of Mesoproterozoic magmatism, sedimentation and terrane amalgamation in southwestern Africa. *S. Afr. J. Geol.* 115, 417–448.

Miyakazi, T., and Shuto, K. (1998). Sr and Nd isotope ratios of twelve GSJ rock reference samples. *Geochem. J.* 32, 345–350. doi:10.2343/geochemj.32.345

Moen, H. F. G. (2001). *Geological map 2818 Onseepkans, 1:250,000*. Council for Geoscience, Pretoria.

Moen, H. F. G., and Toogood, D. J. (2007). *Explanation: sheet 2818: the geology of the Onseepkans area (1:250,000)*. Council for Geoscience, South Africa.

Nke, A. Y., Bailie, R. H., Macey, P. H., Thomas, R. J., Frei, D., Roux, P. L., et al. (2020). The 1.8 Ga Gladkop suite: the youngest Palaeoproterozoic domain in the Namaqua-Natal Metamorphic Province, South Africa. *Precam. Res.* 350, 105941. doi:10.1016/j.precamres.2020.105941

Pettersson, Å., Cornell, D. H., Moen, H. F. G., Reddy, S., and Evans, D. (2007). Ion-probe dating of 1.2 GA collision and crustal architecture in the Namaqua-Natal Province of southern Africa. *Precam. Res.* 158, 79–92. doi:10.1016/j.precamres.2007.04.006

Pettersson, Å., Cornell, D. H., Yuhara, M., and Hirahara, Y. (2009). Sm–Nd data for granitoids across the Namaqua sector of the Namaqua–Natal Province, South Africa. *Geol. Soc. Lon.* 323, 219–230. doi:10.1144/SP323.10

Pettersson, Å. (2008). Mesoproterozoic crustal evolution in South Africa. Ph.D. thesis. Göteborg, Sweden. University of Göteborg.

Raith, J. G., Cornell, D. H., Frimmel, H. E., and De Beer, C. H., (2003). New insights into the geology of the Namaqua Tectonic Province, South Africa, from ion probe dating of detrital and metamorphic zircon. *J. Geol.* 111, 347–366. doi:10.1086/373973

Robb, L. J., Armstrong, R. A., and Waters, D. J. (1999). The history of granulite-facies metamorphism and crustal growth from single zircon U–Pb geochronology: Namaqualand, South Africa. *J. Petrol.* 40, 1747–1770. doi:10.1093/petroj/40.12.1747

Stowe, C.W. (1986). Synthesis and interpretation of structures along the north-eastern boundary of the Namaqua tectonic Province, South Africa. *Trans. Geol. Soc. S. Afr.* 89, 185–198.

Taylor, S. R., and McLennan, S. M. (1995). The geochemical evolution of the continental crust. *Rev. Geophys.* 33, 241–265. doi:10.1029/95RG00262

Thomas, R. J., Agenbacht, A. L. D., Cornell, D. H., and Moore, J. M. (1994). The Kibaran of southern Africa: tectonic evolution and metallogeny. *Ore Geol. Rev.* 9 131–160. doi:10.1016/0169-1368(94)90025-6

Thomas, R. J., Macey, P. H., Spencer, C., Dhansay, T., Diener, J. F. A., Lambert, C. W., et al. (2016). The Sperrgebiet Domain, Aurus Mountains, SW Namibia: a ~2020 to 850 Ma window within the Pan-African Gariep Orogen. *Precambr. Res.* 286, 35–58. doi:10.1016/j.precamres.2016.09.023

Vernon, R. H., Etheridge, M. A., and Wall, V. J. (1988). Shape and microstructure of microgranitoid enclaves: indicators of magma mingling and flow. *Lithos* 22 1–11. doi:10.1016/0024-4937(88)90024-2

Vernon, R. H. (1986). Potassium feldspar megacrysts in granites—phenocrysts, not porphyroblasts. *Earth Sci. Rev.* 23, 1–63. doi:10.1016/0012-8252(86)90003-6

Whalen, J. B., Curries, K. L., and Chappell, B. W. (1987). A-type granites: geochemical characteristics, discrimination and petrogenesis. *Contrib. Mineral. Petrol.* 95, 407–419. doi:10.1007/BF00402202

Whalen, J. B., Jenner, G. A., Longstaffe, F. J., Robert, F., and Gariépy, C. (1996). Geochemical and isotopic (O, Nd, Pb and Sr) constraints on A-type granite petrogenesis based on the Topsails Igneous Suite. *Newfoundland Appalachians. J. Pet.* 37, 1463–1489.

Yuhara, M., Miyazaki, T., Ishioka, J., Suzuki, S., Kagami, H., and Tsuchiya, N. (2002). Rb-Sr and Sm-Nd mineral isochron ages of the metamorphic rocks in the Namaqualand Metamorphic Complex, South Africa. *Gond. Res.* 5, 771–779. doi:10.1016/S1342-937X(05)70912-6

Zhang, K-J., Li, Q.-H., Yana, L.-L., Zeng, L., Lua, L., Zhang, Y.-X., et al. (2017). Geochemistry of limestones deposited in various plate tectonic settings. *Earth Sci. Rev.* 167, 27–46. doi:10.1016/j.earscirev.2017.02.003

Zhang, L.-X., Wang, Q., Zhu, D.-C., Li, S.-M., Zhao, Z.-D.,, Zhang, L.-L., et al. (2019). Generation of leucogranites via fractional crystallization: a case from the Late Triassic Luoza batholith in the Lhasa Terrane, southern Tibet. *Gond. Res.* 66, 63–76. doi:10.1016/j.gr.2018.08.008

**Conflict of Interest:** The authors declare that the research was conducted in the absence of any commercial or financial relationships that could be construed as a potential conflict of interest.